Environmental factors controlling soil organic carbon stability in French forest soils

Laure Soucémarianadin, Lauric Cécillon, Bertrand Guenet, Claire Chenu, François Baudin, Manuel Nicolas, Cyril Girardin, Pierre Barré

Environmental factors controlling soil organic carbon stability in French forest soils

Laure N. Soucémarianadin[1,*], Lauric Cécillon[2], Bertrand Guenet[3], Claire Chenu[4], François Baudin[5], Manuel Nicolas[6], Cyril Girardin[4] and Pierre Barré[1]

[1] Laboratoire de Géologie, PSL Research University, CNRS-ENS UMR8538, Paris, France

[2] Université Grenoble Alpes, Irstea, UR LESSEM, St-Martin-d'Hères, France

[3] Laboratoire des Sciences du Climat et de l'Environnement, LSCE/IPSL, CEA-CNRS-UVSQ, Université Paris-Saclay, Gif-sur-Yvette, France

[4] AgroParisTech-INRA, UMR ECOSYS, Thiverval-Grignon, France

[5] Sorbonne-Université/UPMC, ISTeP, Paris, France

[6] Office National des Forêts, R&D, Fontainebleau, France

* Corresponding author: Laure Soucémarianadin, souce@geologie.ens.fr

Laboratoire de Géologie (UMR 8538) Ecole Normale Supérieure, 24 Rue Lhomond 75231 Paris CEDEX 5, France; phone: +331 44 32 22 94; fax: +331 44 32 22 00

Type: Regular article

Abstract

Aims

In temperate forests, soils contain a large part of the ecosystem carbon that can be partially lost or gained upon global change. Our aim was to identify the factors controlling soil organic carbon (SOC) stability in a wide part of French forests.

Methods

Using a set of soils from 53 French forest sites, we assessed the effects of depth (up to 1 m), soil class (dystric Cambisol; eutric Cambisol; entic Podzol), vegetation types (deciduous; coniferous) and climate (continental influence; oceanic influence; mountainous influence) on SOC stability using indicators derived from laboratory incubation, physical fractionation and thermal analysis.

Results

Labile SOC pools decreased while stable SOC pool increased with depth. Soil class also significantly influenced SOC stability. Eutric Cambisols had less labile SOC in surface layers but had more labile SOC at depth (> 40 cm) than the other soil classes. Vegetation influenced thermal indicators of SOC pools mainly in topsoils (0–10 cm). Mountainous climate forest soils had a low thermal SOC stability.

Conclusions

On top of the expected effect of depth, this study also illustrates the noticeable effect of soil class on SOC stability. It suggests that environmental variables should be included when mapping climate regulation soil service.

Keywords: forest soils, particulate organic matter fractionation, pedology, Rock-Eval 6, soil basal respiration, soil organic carbon persistence

Abbreviations: soil organic carbon (SOC), Rock-Eval 6 (RE6), particulate organic matter (POM), Oxygen index (OI_{RE6}), Hydrogen index (HI), Hydrocarbons (HC)

Introduction

Forest ecosystems play a central role in the global carbon (C) cycle with their high potential for atmospheric CO_2 sequestration (Intergovernmental Panel on Climate Change 2000; Smith et al. 2014). About half of the terrestrial C sink is indeed located in forests (Canadell et al. 2007) and forest soils in particular store around 398 Pg C (Kindermann et al. 2008). The temperate biome holds a quarter of the world's forests (Tyrrell et al. 2012) and soils in temperate forests have twice as much carbon as the vegetation (Jarvis et al. 2005). Temperate forest soils have also constituted a C sink for over two decades (Pan et al. 2011; Tyrrell et al. 2012) with parts of the European—and particularly French (Jonard et al. 2017)—forest soils being particularly efficient at sequestering C (*e.g.*, Nabuurs et al., 2008). The contribution of deep soil to soil organic carbon (SOC) stocks has been previously highlighted (Jobbágy and Jackson 2000; Rumpel and Kögel-Knabner 2010), however there is still a lack of data on deep/subsoil mineral (> 30 cm depth) SOC stocks (*e.g.*, Tyrrell et al. 2012).

SOC is made up of very heterogeneous compounds (Amundson 2001; Trumbore 1997) with turnover times ranging from a few days/weeks to several centuries and, for modelling

purposes, can be roughly divided into active (labile), intermediate and passive (persistent) SOC kinetic pools.

Labile SOC is the most likely to be quickly affected by climate or land-use changes (Carter et al. 1998; Zhang et al. 2007), thus potentially contributing further to global warming. Moreover, because of the central role of the SOC labile pool in short-to medium-term nutrient availability and soil structural stability (Wander 2004), its evolutions could have major effects on biomass (food/timber/etc.) production. Conversely when considering SOC long-term storage and possible sequestration, soils in which most of the total SOC is stable will perform better than soils with a greater proportion of their total SOC as labile SOC (Jandl et al. 2007; Lorenz and Lal 2010; Prescott 2010). It is thus essential to determine how much labile and persistent SOC are present in soils.

Despite being of such interest, there is still no standard technique to assess SOC stability but a set of complementary techniques are available. Respiration measurements and particulate organic matter (POM) quantification obtained by various methods of fractionation (density only / density + particle-size) (von Lützow et al. 2007) have been used for decades and are traditional metrics of SOC lability. Although the respired-C and POM-C fractions both represent a labile SOC pool, the former corresponds to a smaller SOC pool with a shorter mean residence time (usually < 1 year for temperate in-situ conditions) (Feng et al. 2016) while the latter corresponds to a larger SOC pool with a longer mean residence time (usually < 20 year for temperate conditions (*e.g.*, Balesdent 1996; Trumbore et al. 1996). This longer residence time may result from interactions with the soil structure; part of the POM-C fraction being occluded in micro-aggregates and protected from microbial respiration for longer time scales (Six et al. 2002). The mean residence time of the POM-C fraction can also exceed 20 years, especially in cold and mountainous areas (Leifeld et al. 2009) or in areas affected by wildfires where the POM-C fraction may contain large amounts of pyrogenic carbon with

97 residence time in soils greater than the mean residence time of total SOC. Nevertheless, it has
98 been shown that the POM-C fraction of temperate and mountainous soils of agroecosystems
99 correspond roughly to the resistant material pools (RPM) of the RothC model (Zimmerman et
100 al. 2007), which has a turnover rate of 3 years (Coleman and Jenkinson 1999). In this paper,
101 the respired-C fraction will be referred to as the highly-labile SOC pool and the POM-C
102 fraction will be termed labile SOC pool.
103 Thermal analysis techniques have also been used to characterize soil organic matter (SOM)
104 stability (*e.g.*, Plante et al. 2009). Among them, Rock-Eval 6 (RE6) analysis has shown
105 promising results in the determination of SOM biogeochemical stability (Barré et al. 2016;
106 Gregorich et al. 2015; Saenger et al. 2015; Sebag et al. 2016). RE6-derived parameters are
107 reliable indicators of the stable SOC pool (Barré et al. 2016; Cécillon et al. 2018) and can be a
108 useful complement to the aforementioned usual indicators of the labile SOC pool
109 (Soucémarianadin et al. 2018). Specifically, one RE6-derived parameter, $T_{50\_HC\_PYR}$, which
110 corresponds to the temperature at which 50% of the hydrocarbons released as pyrolysis
111 effluents during SOM pyrolysis have evolved, was linked to the highly-labile and the labile
112 SOC pools (Gregorich et al. 2015; Soucémarianadin et al., 2018). In French forest soils,
113 $T_{50\_HC\_PYR}$ was shown to be strongly and negatively correlated to the POM-C fraction but not
114 to the respired-C fraction (Soucémarianadin et al. 2018). $T_{50\_HC\_PYR}$ could thus be used as an
115 indicator of the labile SOC pool defined above, similarly to the POM-C fraction. Another
116 RE6-derived parameter, the temperature at which 50% of the CO_2 resulting from SOM
117 thermal oxidation has evolved ($T_{50\_CO2\_OX}$) was positively related to an increasing proportion
118 of persistent SOC (Barré et al. 2016; Cécillon et al. 2018) and to a POM-C depletion in
119 temperate forest soils (Soucémarianadin et al. 2018). $T_{50\_CO2\_OX}$ could thus be used as an
120 indicator of the stable SOC pool with mean residence times greater than several decades (>
121 50–100 years; Cécillon et al. 2018).

Few studies have assessed the factors controlling SOC stability over large areas. Several recent studies have highlighted the importance of parent material and soil type on SOC content and stability, SOC in deep soil layers being generally more stable compared to surface SOC (Barré et al. 2017; Mason et al. 2016; Mathieu et al. 2015; Mulder et al. 2015). Camino-Serrano et al. (2014) reported a larger highly labile SOC pool (based on concentrations of dissolved organic carbon; DOC) in soils types characterized by a very acidic pH than in more basic soils, especially in the subsoil layers below 20 cm depth. Considering croplands and grasslands in Germany, Vos et al. (2017) showed that sandy soils had a larger labile SOC pool (POM-C fraction) than soils with finer texture.

Land cover and vegetation type have also been shown to strongly control SOC stability. Wiesmeier et al. (2014) found lower proportions of stable SOC pool in Bavarian forests compared to grasslands or croplands, confirming results across Europe that showed that afforestation of cropland and grassland generally decreased SOC stability (Poeplau and Don 2013). In the temperate forests of Bavaria, vegetation type was also shown to control SOC stability, coniferous forests having higher labile SOC proportions than deciduous and mixed forests (Wiesmeier et al. 2014). Similar results were obtained for the highly labile SOC pool with lower dissolved organic carbon concentrations in broadleaved forests than coniferous forests (Camino-Serrano et al. 2014). Variations of soil respiration were also observed at the species level (*e.g.*, three species of oaks; You et al. 2016).

Regarding climate, both global and more local studies have highlighted the strong positive relationship with precipitation and the negative effect of temperature on SOC quantity (Jobbágy and Jackson, 2000; Paul et al., 2002; Callesen et al., 2003; Wiesmeier et al. 2013). Labile OM and particularly the POM-C fraction, has been shown to dominate in soils located at higher elevations and experiencing colder mean annual temperatures (*e.g.*, Leifeld et al. 2009; Sjögersten et al. 2011). Considering over 300 forested sites, higher DOC concentrations

147 (highly labile SOC pool) were found in temperate sites than boreal and tropical sites (Camino-
148 Serrano et al. 2014). To the exception of the work of Wiesmeier et al. (2014), we are not
149 aware of large scale studies that would consider both the highly labile, labile and stable SOC
150 pools and devoted to forest soils, despite their large SOC stocks.
151 The objectives of the study were thus to assess the importance of various environmental
152 factors, soil depth, soil class, vegetation type and climate class in controlling the stability of
153 SOC in forest soils. To this purpose, we used a set of complementary techniques, namely the
154 Rock-Eval 6 thermal analysis, POM separation by size and density and a laboratory 10-week
155 incubation, and applied them to a large set of French forest soil samples that covers a large
156 pedoclimatic variability, a wide tree species diversity and includes deep samples (up to 1
157 meter).
158 We hypothesized that 1/ SOC stability would vary with depth with surface soil layers
159 containing more labile SOC while deep soil layers would contain more stable SOC; 2/
160 vegetation type would influence SOC stability mostly in surface soil layers (with higher rates
161 of C input from plants), SOC being more labile in topsoils of coniferous forests; 3/ soil class
162 would influence SOC stability mostly in medium/deep soil layers (below 20 cm); and 4/
163 climate would influence SOC stability and SOC in mountainous plots would be more labile.
164

165 ## Material and methods

166 a. Sites and soil samples

167 We considered forest mineral soil samples from 53 permanent forest sites of the French
168 national network for the long term monitoring of forest ecosystems (‘‘RENECOFOR’’),
169 established in 1992 (Ulrich 1995) by the National Forest Service (ONF;
170 http://www.onf.fr/renecofor) as a part of the European ICP-FORESTS (http://icp-forests.net/)
171 level 2 network (Fig. 1a). Our selected sites are variable in terms of climate (continental

influence; oceanic influence; mountainous influence; with mean annual precipitation MAP and mean annual temperature MAT ranging between 703–1894 mm and 4.8–12.3 °C respectively for the 1971–2000 period), soil type with a class constituted of soils related to entic Podzols, another class constituted of eutric and epileptic Cambisols as well as Calcisols and a last class constituted of dystric and hyperdystric Cambisols (IUSS Working Group 2015) and forest vegetation with coniferous [silver fir (*Abies alba* Mill.); Norway spruce (*Picea abies* (L.) H. Karst.); European larch (*Larix decidua* Mill.); Scots pine (*Pinus sylvestris* L.)] and deciduous [beech (*Fagus sylvatica* L.); sessile (*Quercus petraea* (Matt.) Liebl.) and/or pedunculate oaks (*Quercus robur* L.)] stands. Stands are even-aged.

At each site, samples representing five soil layers were obtained (0–10 cm, 10–20 cm, 20–40 cm, 40–80 cm and 80–100 cm; Fig. 1b). Samples of the first three top soil layers were collected, at each depth, as 5 (replicates; pooled together on site) × 5 (sub-plots) sampling points over the 5000 m^2 central plot, by progressively digging a 50 cm wide soil profile (Jonard et al. 2017; Ponette et al. 1997). This sampling campaign took place between 2007 and 2012. Samples of the two deeper soil layers were taken from two soil pits located just outside the central plot and collected in 1994–1995 (Brêthes et al. 1997).

Bulk soils were air-dried and stored in plastic buckets right after sampling. One liter of soil of each layer was retrieved for this study by isovolumetrically pooling the samples of the 5 subplots (200 mL each) for the first three layers (0–40 cm) and the 2 faces of the 2 soil pits (250 mL each) for the two deepest layers (40–100 cm). The pooled samples were sieved at 2 mm before analysis.

b. Elemental analysis

Bulk < 2 mm-sieved soil samples were ground (< 250 µm; ultra-centrifugal mill ZM 200, Retsch Gmbh) and organic carbon and total nitrogen concentrations were determined by dry

197 combustion with an elemental analyzer (CHN NA 1500, Carlo Elba). Samples with
198 carbonates (total $CaCO_3$ = 3.5–835 $g \cdot kg^{-1}$) were first decarbonated following the same
199 protocol as Harris et al. (2001). Briefly, 30 mg of ground samples were weighed in 5 mm × 9
200 mm silver boats followed by the addition of 50 µL of distilled water. The boats were put in a
201 glass bell jar, next to a beaker containing 100 mL of concentrated HCl (12 $mol \cdot L^{-1}$). The air
202 in the jar was evacuated and samples let to sit in this HCl-saturated atmosphere to allow the
203 acid to dissolve water and hydrolyze the carbonates for 8 h. Then, the decarbonated samples
204 were dried at 60 °C in the silver boats for at least 48 h. Silver boats were further placed in 10
205 mm × 10 mm tin boats and analyzed for C and N.
206 POM fractions (see subsection d) were ground with a ball mill (mixer mill MM 200, Retsch
207 Gmbh) or a mortar and pestle when the sample mass was less than 0.05 g. Carbon
208 concentration was determined as for the bulk soil.
209
210 c. Respiration test
211 For each sample, 20 g of 2 mm-sieved soil were transferred in a 120 mL glass-flask and re-
212 humected at pF 2.5 (−0.033 MPa), which had been previously determined using a 5 Bar
213 pressure plate extractor (#1600, Soilmoisture Equipment Corp.). The flasks were fitted with
214 aluminum seals with PTFE-faced silicone septa to allow for headspace gas sampling and
215 placed inside an incubator (AE240 BIO EXPERT, Froilabo SAS) kept at 20 °C for 10 weeks
216 following a two-week period pre-incubation to allow the samples microbial activity to
217 stabilize (data not included).
218 Headspace gases were sampled at 1 to 2-week intervals during the 10-week incubation period
219 and CO_2 concentrations were determined using an Agilent 490 micro-gas chromatograph
220 equipped with the OpenLAB Chromatography Data System EZChrom software.

When CO_2 concentrations had reached 2.5–3% or was expecting to do so before the next measurement, and/or when the cap had been pierced with the needle four times, flasks were opened and flushed with fresh and moist air to return CO_2 concentrations to ambient levels to avoid anoxia (while maintaining the moisture content), before returning them to the incubator. The CO_2 released during the incubation experiment was expressed as the cumulated soil microbial respiration rate (basal respiration) from the initial SOC content over the 10-week period, or the 10-week mineralizable SOC (respired-C) and reported as a percentage of total SOC to account for differences in the C content of the various layers and sites. Respired-C was used as indicator of the highly labile SOC pool with mean residence time below 1 year.

d. Particle size and density SOC fractionation

To isolate the particulate organic matter (POM) fraction, samples were first dried at 50 °C for 24 h before weighing 25 g and transferred them in polyethylene (PE) 250 mL flasks. We then added 180 mL of 0.5% sodium hexametaphostate solution and ten 5 mm-diameter glass beads before shaking the samples overnight (50 rpm; 16 h) on an overhead shaker (Reax 2, Heidolph). Samples were thoroughly rinsed over a 50-µm mesh with deionized water. The sand fraction was then transferred back to a dry PE flask with a sodium polytungstate (SPT) solution of density = 1.6 ± 0.03 g·cm^{-3} (Crow et al. 2007; Golchin et al. 1994) and solution was added up to around 180 mL. The flasks were shaken overhead by hand 10 times and samples were left overnight to settle down after the cap of the flask was rinsed with the SPT solution. The floating material was collected with a spatula and placed over a 50-µm mesh sieve. If necessary some SPT solution was added back to the flask and the previous step was repeated. This time, samples were placed in a centrifuge for 30 minutes to accelerate the separation (2750 rpm or 1250 g). The floating material was again collected with the spatula or pipetted depending on the amount left. This step was repeated if the light fraction was

abundant. If not, samples were left to settle down overnight before one last collection. The POM fraction on the sieve was thoroughly rinsed with deionized water throughout the whole process. The sieves and fractions were then placed in the oven at 50 °C for 24 h before being weighed. To account for differences in the C content of the different samples, we calculated the proportion of OC in the POM fraction (POM-C), expressed as a percentage of total SOC. POM-C was used as indicator of the labile SOC pool with mean residence time generally up to 20 years.

e. Thermal analysis: Rock-Eval 6

The thermal analysis of the samples was performed with a Rock-Eval 6 turbo device (Vinci Technologies, France). Details about the equipment have been previously published (Behar et al. 2001). We adapted the procedure developed for the analysis of SOM by Disnar et al. (2003). Briefly, about 60 mg of ground sample were exposed to two consecutive thermal treatments, first in a pyrolysis oven (200–650 °C; thermal ramping rate of 30 °C·min^{-1}; under N_2 atmosphere) then in a combustion oven (300–850 °C; thermal ramping rate of 20 °C·min^{-1}; under laboratory air atmosphere). At the beginning of the pyrolysis, there was an isothermal step (at 200 °C) during ≈ 200 seconds during which the free hydrocarbons (HC) were thermovaporized (S1 peak). The pyrolysis effluents (mostly HC) were detected and quantified with flame ionization detection, while CO and CO_2 were quantified by infrared detection during both the pyrolysis and oxidation stages (Online Resource 1).

Two standard RE6 parameters describing SOC bulk chemistry were determined: the hydrogen and oxygen indices (HI and OI_{RE6}). The HI index corresponds to the amount of hydrocarbons formed during thermal pyrolysis of the sample (HC evolved between 200 and 650 °C minus the S1 peak) divided by the total SOC content of the sample and is expressed in mg HC·g^{-1} SOC. It describes the relative enrichment/depletion of SOC in hydrogen-rich moieties. The

OI_{RE6} index describes the relative oxidation status of SOC. It was calculated using the equation proposed by Lafargue et al. (1998):

$$OI_{RE6} = 16 / 28 \times OI_{CO} + 32 / 44 \times OI_{CO2} \quad \text{(equation 3)}$$

Where OI_{CO2} corresponds to the CO_2 yielded during thermal pyrolysis of the sample between 200 and 400 °C divided by the total SOC of the sample and OI_{CO} corresponds to the CO yielded during thermal pyrolysis between 200 and 400–650 °C (wherever a minimum of CO production is observed; in the absence of a minimum, the default upper-limit temperature is set at 550 °C) divided by the total SOC of the sample. Thus OI_{RE6} is expressed in mg $O_2 \cdot g^{-1}$ SOC.

We derived two additional RE6 parameter describing the thermal stability of SOC: (i) $T_{50\_HC\_PYR}$, the temperature at which 50% of the HC resulting from the SOM pyrolysis had evolved and (ii) $T_{50\_CO2\_OX}$, the temperature at which 50% of the CO_2 resulting from the SOM oxidation had evolved. The upper limit temperature for the integration of this signal was set at 611 °C to obtain a total CO_2 signal evolved from pure OM without interference of carbonates. $T_{50\_HC\_PYR}$ was used as an indicator of the labile SOC pool with mean residence time generally up to 20 years (negative correlation with the labile SOC pool according to Gregorich et al. (2015) and Soucémarianadin et al. (2018)), while $T_{50\_CO2\_OX}$ was used as an indicator of the stable SOC pool with mean residence time typically greater than 50–100 years, following Barré et al. (2016) and Cécillon et al. (2018). Signal processing of the RE6 thermograms, *i.e.*, signal integration and calculation of $T_{50\_HC\_PYR}$ and $T_{50\_CO2\_OX}$, was performed with the R environment software v.3.3 (R Core Team 2016) using the hyperSpec (Beleites and Sergo 2015) and pracma (Borchers 2015) R packages.

f. Calculations and statistical analyses

For the respiration test, samples with very low C content (< 0.2%) were not considered as the C respired during the incubation period was too close to the limit of detection for reliable determination. For the thermal analysis, we used a C content threshold of 0.1% and manually inspected the pyrolysis thermograms for samples with 0.1% ≤ C content ≤ 0.25% to make sure of the validity of the RE6 data (by assessing the shape of the signal). This resulted in the selection of n = 46 / 50 and n = 31 / 33 samples for the soil layers 40–80 cm and 80–100 cm and the two methods respectively, leading to a total n = 236 for respiration test and n = 242 for RE6 (Fig. 1b). Because POM fractionation is time-consuming, we analyzed only the soil layers 0–10 cm and 40–80 cm (Fig. 1b). At two sites, soil was too shallow (< 40 cm) and no sample was therefore collected for the 40–80 cm layer, and we used the same C threshold as for the RE6 to select the POM samples, which lead to n = 103. Out of the 236 samples considered for the respiration test, 35 had a $CaCO_3$ content over 5% (5.2–82.0%). We tested the correlation between respired-C and $CaCO_3$ content and, as it was not significant, decided to proceed with the statistical analysis with all the samples.

Basic soil parameters (pH, texture, cation exchange capacity) were previously published in Ponette et al. (1997). Average values are reported in Table 1 as well as the C content and C/N ratio measured on the composite samples from this study. Because we used isovolumetric pooled sampled, we saw appropriate to use average values of the 5 replicates × 5 sub-plots. This was confirmed by the results we obtained for the C content (Online Resource 2).

Relationships between the indicators of SOC stability and soil physico-chemical properties as well as climatic data (MAT and MAP) were estimated using Spearman rank correlation as the data did not meet the assumption of normality. Correlations were also performed on different sets of samples for the different indicators (233 samples were included for the respiration test, 242 for the RE6 comparison and 103 for the POM fractionation).

A principal component of analysis (PCA) was performed to illustrate linear relations between the indicators derived from the 3 methods at two different depths: 0–10 cm and 40–80 cm. For that purpose, data were log-transformed, centred and scaled. To determine the number of principal components to select, we looked at the percentage of the total variance explained and used a scree plot and Kaiser's criterion. We projected the physico-chemical and climatic variables on the circle of correlations to see if any of those was associated with either of the principal components and could thus be associated with SOC stability.

The statistical analysis to determine the driving factors of SOC stability was performed in two steps: first over the complete soil profile and then on each soil layer individually. We used multivariate models to assess the effects of the different environmental factors on the RE6-based parameters and respiration test and POM fractionation results. For this "analysis by soil profile", we used linear mixed models introducing a random intercept for each site (≈ to treat "site" as random effect) to take into account that the different layers constituted repeated measures (increasing depth within a same RENECOFOR site). To do so we added the compound symmetry structure, which is similar to the variance structure of random-intercept-only model, to a generalized least squares function (that fits a linear model using generalized least squares; (Pinheiro et al. 2016)). Model selection was then implemented with a top-down strategy. The response variables were transformed, to the exception of $T_{50\_HC\_PYR}$ and $T_{50\_CO2\_OX}$, using the Box-Cox transformation technique ($\log_{10}$ for POM-C and (respired-C + 1)), as they showed evidence of the variance increasing with the mean response. After transformation, the residuals followed an approximate normal distribution.

To explore further the effects of soil classes, vegetation types and climatic zones within each layer, we then conducted three-way analyses of variance (ANOVA) "by layer" with type II analysis, when the interactions were not significant. Data were not transformed except for respired-C. Multiple comparison tests were performed with Tukey's honest significant

differences (to get adjusted *p*-values for all comparisons) and pairwise t-test (no adjustment method). All comparisons were considered significant at an alpha value (α) of 0.05.

All statistical analyses were performed using the R 3.3 statistical software (R Core Team 2016) with the factoextra (Kassambara and Mundt 2016), nlme (Pinheiro et al. 2016), lme4 (Bates et al. 2015) and car (Fox and Weisberg 2011) packages.

Results

a. Highly labile SOC pool: respired-C

Depth and soil class significantly influenced variations in soil basal respiration (respired-C) across our 53 study plots. The depth × soil interaction was also included in the selected model ($p = 0.042$; Online Resource 3). The respired-C fraction was on average 1.46 ± 0.63% of total SOC (Online Resource 4) with no significant differences among vegetation types (Fig. 3) or climatic zones (Table 2). Respired-C decreased with depth (Fig. 2) but that factor was only marginally significant. Soil class was not significant in the 40–80 cm layer but otherwise entic Podzols had significantly lower respired-C than the two other soil classes ($p = 0.0010$–0.042; Table 2; Fig. 4).

b. Labile SOC pool: POM-C and $T_{50\_HC\_PYR}$

Only depth and soil type significantly affected variations in POM-C across our 53 study plots (Online Resource 3). The labile SOC fraction contained in POM decreased by almost half from the 0–10 cm layer to the 40–80 cm layer (with respective proportions of 22.6 ± 7.3% and 11.5 ± 6.2% of total SOC; Fig. 2). The analysis by layer confirmed that neither climate nor vegetation significantly influenced POM-C variations (Table 2; Fig. 3). Eutric Cambisols had

significantly less POM-C than entic Podzols in the surface layer and dystric Cambisols at 40–80 cm (Fig. 4; Online Resource 4).

Depth, vegetation type and soil class influenced variations in $T_{50\_HC\_PYR}$, the RE6-derived temperature at which 50% of the HC resulting from the SOM pyrolysis had evolved. The three interactions depth × soil, depth × veg and soil × veg were also included in the selected model (Online Resource 3). $T_{50\_HC\_PYR}$ significantly increased with depth (422 ± 8 to 452 ± 13 °C at 0–10 cm and 80–100 cm, respectively; Fig. 2), illustrating the decrease of the labile SOC pool with increasing depth. Eutric Cambisols had significantly higher $T_{50\_HC\_PYR}$ than dystric Cambisols and entic Podzols in the surface layer but had significantly lower $T_{50\_HC\_PYR}$ than the two other soil classes at 20–40 cm depth (Fig. 4; Online Resource 4). Moreover, in the surface layer, samples in deciduous plots had a significantly higher $T_{50\_HC\_PYR}$ than those in coniferous plots (427 ± 9 and 417 ± 7 °C, respectively, $p < 0.001$; Table 2; Fig. 3).

c. Stable SOC pool: $T_{50\_CO2\_OX}$

Depth, vegetation and climate induced significant variations in the temperature at which 50% of the CO_2 resulting from the SOM oxidation had evolved ($T_{50\_CO2\_OX}$) across our 53 study plots. The depth × climate interaction was also included in the selected model (Online Resource 3).

$T_{50\_CO2\_OX}$ increased with depth (from 399 ± 9 to 437 ± 19 °C at 0–10 cm and 80–100 cm, respectively; Fig. 2). Vegetation type was significant only in the top soil layers (0–40 cm) with samples from coniferous plots having a lower $T_{50\_CO2\_OX}$ than those in deciduous plots (395 ± 6 °C and 405 ± 9 °C, respectively; Fig. 3). Soil class was a significant factor both in layers 0–10 cm ($p = 0.0085$) and 40–80 cm ($p = 0.0489$; Table 2) but with contrasting trend: in the surface layer, eutric Cambisols had the highest $T_{50\_CO2\_OX}$ (significantly higher than

392 entic Podzols) and the lowest $T_{50\_CO2\_OX}$ in the 40–80 cm layer (significantly lower than the
393 dystric Cambisols; Fig. 4; Online Resource 4). Climate was a significant factor in all layers:
394 over the whole profile (0–100 cm), $T_{50\_CO2\_OX}$ was lower in mountainous plots than in plots
395 located in the two other climate classes ($p \leq 0.0001$–0.0159; Table 2; Fig. 5).
396
397 d. Correlations between soil and climate characteristics and the indicators of SOC stability
398 There were only a few significant and strong correlations between the indicators of SOC
399 stability and soil physico-chemical properties (Table 3). Notably POM-C and $T_{50\_HC\_PYR}$, the
400 two indicators of the labile SOC pool, had strong and opposite correlations with HI ($\rho = 0.67$
401 and -0.67 respectively) and OI_{RE6} ($\rho = -0.76$ and 0.63 respectively). POM-C was also
402 positively correlated with C/N ratio ($\rho = 0.61$). $T_{50\_CO2\_OX}$ was negatively correlated to the C
403 content ($\rho = -0.72$; Table 3). Respired-C showed no strong correlation with soil or climate
404 characteristics. In our samples we observed no strong correlation for the four indicators of
405 SOC stability with soil texture, pH (although $\rho = -0.54$ with POM-C) or the climatic
406 characteristics (MAT or MAP; Table 3).
407 Because of the strong "depth effect" on each indicator of SOC stability, we explored the
408 evolution of these correlations within each soil layer and noticed that they also evolved with
409 depth (Online Resource 5). To describe the similarity or dissimilarity in the different
410 indicators of SOC lability, we conducted a principal component analysis (PCA) at the two
411 depths for which POM-C was available (0−10 and 40−80 cm). In the 0−10 cm layer, the first
412 two principal components (PC) explained almost 60% of the total variance (Fig. 6). PC1
413 clearly separated soil samples dominated by highly labile SOC pool from those dominated by
414 labile SOC pool associated with POM-C. Indeed, along PC1, POM-C and respired-C showed
415 moderate to strong negative and positive loadings respectively, while $T_{50\_CO2\_OX}$ had moderate
416 positive loadings (Fig. 6). $T_{50\_HC\_PYR}$ showed strong negative loadings along PC2, while it had

very weak negative loadings along PC1. Results were quite different in the 40−80 cm layer, where the first two principal components (PC) explained approximately 63% of the total variance (Fig. 6). In these deeper samples, PC1 tightly grouped soil samples with high proportion of highly labile SOC pool (respired-C) and those with high proportion of labile SOC pool associated with POM-C with strong positive loadings for both indicators along PC1. $T_{50\_CO2\_OX}$ and $T_{50\_HC\_PYR}$ had both strong positive loadings along PC2, while they had very weak loadings along PC1.

SOC content was not related to any of the indicators of SOC stability in the surface layer, while it was moderately and negatively correlated with POM-C, respired-C and $T_{50\_CO2\_OX}$ in the deep layer (Fig. 6; Online Resource 5). In the surface layer, pH was associated with positive values on the first PC (high respired-C), while sand content and soil C/N ratio were associated with negative values on the first PC (high POM-C; Fig. 6; Online Resource 5). HI and OI_{RE6} were well correlated to the indicators of highly labile and labile SOC pools, specifically in the surface layer. Correlations of the physico-chemical variables with POM-C were slightly lower at depth (Online Resource 5), but below 20 cm depth, all these correlations with $T_{50\_HC\_PYR}$ and respired-C (directly with the indicators or with the PCs) had greatly decreased or even disappeared (Online Resource 5). Conversely, $T_{50\_CO2\_OX}$ was not more than weakly correlated with the physico-chemical parameters over the whole profile but its positive correlation with MAT tended to be higher in deeper layers (Online Resource 5; Fig.6).

The PCA biplot displaying the samples based on their soil class (Fig. 6) showed a difference between eutric Cambisol and entic Podzol with the two first PCs in the surface layer (0–10 cm): samples of eutric Cambisols had higher respired-C, lower POM-C and generally higher $T_{50\_HC\_PYR}$ and $T_{50\_CO2\_OX}$ than those of entic Podzols.

In the deep layer (40–80 cm), the two PCs separated samples of dystric Cambisols from samples of eutric Cambisols. The former were mostly characterized by high respired-C and POM-C values and high values of $T_{50\_HC\_PYR}$ and $T_{50\_CO2\_OX}$. The latter had either high values of $T_{50\_HC\_PYR}$ and $T_{50\_CO2\_OX}$ with low respired-C and POM-C or low values of $T_{50\_HC\_PYR}$ and $T_{50\_CO2\_OX}$ with high respired-C and POM-C. The second PC separated samples that had more stable SOC (high values on PC2) from those that had less stable SOC (low values on PC2). Dystric Cambisols thus appeared as having more stable SOC than the two other soil classes (Fig. 6).

Discussion

a. Depth is the most discriminating factor of SOC stability

In our study sites, depth was the most discriminating factor, affecting significantly all indicators of SOC stability. Indeed, with depth, we observed consistent trends for the indicators of the highly-labile (decrease of respired-C) and the labile (decrease of POM-C and increase of $T_{50\_HC\_PYR}$) SOC pools, and an opposite trend for the indicator of the stable SOC pool (increase of $T_{50\_CO2\_OX}$), verifying our first hypothesis.

Studies have shown a decrease in POM-C (% of total SOC) with increasing depth down to 20–30 cm (Hassink 1995; Schrumpf and Kaiser 2015), down to 50 cm (Diochon and Kellman 2009) or down to > 140 cm (Cardinael et al. 2015; Moni et al. 2010). Previous studies have also reported decreasing respired-C with depth during incubations of variable duration (*e.g.*, Dodla et al. 2012; Gillespie et al. 2014; Schrumpf et al. 2013; Wang and Zhong 2016 with 12 days at 22.5 °C, 20 days at 15 °C, 98 days at 25 °C, 60 days at 25 °C, respectively). Variations in soil basal respiration with depth have been related with variations in C dynamics (*e.g.*, Agnelli et al. 2004; Salomé et al. 2010; Wordell-Dietrich et al. 2017).

Labile SOC content usually decreases while stable SOC increases with depth (*e.g.*, Jenkinson et al. 2008; Lorenz and Lal 2005; Mathieu et al. 2015) and this is correlated with longer SOC turnover rates as exemplified by Torn et al. (1997) and Mathieu et al. (2015) who showed strong effects of depth on SOC mean age.

b. Soil class as a major factor controlling SOC stability

Soil class had significant effects on the indicators of the highly-labile (respired-C) and labile (POM-C and $T_{50\_HC\_PYR}$) SOC pools. Contrary to our third hypothesis, these soil effects were not limited to the deeper layers and were indeed present in the surface layer for all four indicators of SOC stability (Table 2).

i) Modulation of the effect of depth by soil class

The effect of depth on SOC stability, *i.e.* the decrease of the labile SOC and concomitant increase in stable SOC was modulated by the soil class. First, the surface (0-10 cm) values of all SOC stability parameters varied among soil classes (Table 2; Fig. 4), surface layers of eutric Cambisols being generally enriched in stable SOC compared to other soil classes. This might be explained by a relative higher stabilization of SOC in the surface layer of the eutric Cambisols that could be due to a faster cycling in relation to lower C/N ratios (13.2 ± 1.5 vs. 18.4 ± 4.5 for the other two classes) and higher pH (6.2 ± 0.9 vs. 4.3 ± 0.3 for the other two classes), stimulating the mineralization of the more labile SOC and resulting in a more stable SOC overall. SOC stabilisation through Ca-mediated processes (occlusion, inclusion, sorption; Rowley et al., 2018) may also explain the higher SOC stability in surface layers of eutric Cambisols.

Then the amplitude of the evolution of SOC stability with depth varied among soil classes (Figure 4). Thus, the higher stability observed in the surface layer of eutric Cambisols had disappeared by 20–40 cm depth. This modulation of the effect of depth by soil class could be

linked to different types of SOM moieties developed by very different pedogenetic processes, eutric Cambisols showing a relatively more oxidized SOC than other soil classes (higher OI_{RE6}; specifically down to 40 cm depth). In the deep layer, dystric Cambisols were characterized by high OI_{RE6} values, which could be linked to larger stable SOC pools in this soil class, likely associated with more oxidized SOC moieties (Cécillon et al., 2018). Lastly, in our sites, soil class did not significantly affect the indicator of stable SOC ($T_{50\_CO2\_OX}$; at least not for the whole profile model), and the stable SOC pool appeared mostly driven by differences in MAT (specifically at depth; Fig 6; see section d. of the Discussion). This result is seemingly contradictory to the findings of Mathieu et al. (2015) who reported a strong influence of soil type on deep soil mean carbon age. It should be noted that these authors covered a greater soil variability in their study and if we focus on the 3 soil classes considered in our work, their results are similar to ours (*i.e.*, no large difference among the three soil classes).

ii) Soil variables explaining the pedological effect on SOC stability

Soil type is not often used as an explanatory factor of variations in SOC quality/stability (*e.g.*, Wiesmeier et al. 2014) and physico-chemical properties (*e.g.*, clay content, pH, etc.) are often preferred (*e.g.*, Tian et al. 2016). We thus wondered whether a series of physico-chemical parameters could have summarized the soil class effect on SOC stability.

The effect of soil type on the highly-labile and labile SOC pools may be due to differences in soil texture (sand content), pH or C/N ratio (Online Resource 6, Fig. 6). Indeed, a strong effect of soil texture on SOC stability in the topsoil (0–10 cm) has previously been reported in the literature. For instance, just like we did (POM-C in coarse-textured entic Podzols = 25.1 ± 7.6% vs. 19.2 ± 5.6% in fine-textured eutric Cambisols; Fig. 4; Online Resource 4), several studies have observed a trend of more labile SOC (expressed as POM-C or size of the

intermediate SOC pool) in coarser soils (Schiedung et al. 2017; Wiesmeier et al. 2014) or directly linked to the sand fraction (Tian et al. 2016; Vos et al. 2017).

In our sites, respired-C was higher in fine-textured soils up to 40 cm depth and was significantly lower in Podzols. Conversely, several studies have reported higher C mineralization rates in sandy soils than in finer-textured soils in various contexts from boreal forests through croplands in Norway and all the way to Brazil (Bauhus et al. 1998; Frøseth and Bleken 2015; Schmatz et al. 2017). These opposite results could originate from various sources, and specifically differences in C/N ratio. For our sites, the topsoil C/N ratio in eutric Cambisols was significantly lower (13.3 ± 1.5) than in entic Podzols (19.9 ± 5; Online Resource 4), which could affect the microbial use efficiency during the incubation (*e.g.*, Cotrufo et al. 1995). Differences in pH could be another good explanation. Our entic Podzols and eutric Cambisols had lower and higher pH than the till (≈ sandy) and clay soils from the Bauhus et al. (1998) study, respectively. It has been shown that a slight increase in pH could significantly increase rates of mineralization (Curtin et al. 1998).

All these physico-chemical variables reflect the importance of SOM stoichiometry (C/N ratio) (Ågren et al. 2013; Cleveland and Liptzin 2007) and substrate accessibility (reduced protection via aggregation in sandy soils or increase in dissolved OM with higher pH) for its degradation (Dungait et al. 2012; Schmidt et al. 2011). However the lack of or low to moderate correlations between the different indicators of SOC stability and these soil physico-chemical parameters (texture and pH respectively; Table 3) suggest that there is not one characteristics only responsible for the soil effect we observed or that, at least, they are not valid at all depths of the soil profile as we have shown (Online Resource 5; Fig. 6). There are likely complex interactions, reflecting pedogenetic processes behind this and, in that regard, the soil class is integrative and goes beyond simple soil physico-chemical characteristics, and is thus capable of reflecting variations in SOC stability.

539

540 c. Vegetation type mostly affects SOC stability in topsoils

541 In our study sites, the effect of vegetation type (coniferous forest *vs*. deciduous forest) on
542 SOC stability was concentrated on the surface layer (0–10 cm), thus validating part of our
543 second hypothesis. Vegetation type significantly influenced both thermal indicators of SOC
544 stability in surface soil layers while the classical indicators of the highly labile (respired-C)
545 and the labile (POM-C) SOC pools were not affected by vegetation.

546 Effects of vegetation on the labile SOC pool have been previously reported, but they were
547 mainly observed at the tree species level (Bauhus et al. 1998; Augusto et al. 2002; Hobbie et
548 al. 2007; Olsen and Van Miegroet 2010; Laganière et al. 2012; Vesterdal et al. 2012; You et
549 al. 2016). Conversely, previous studies have also reported a lack of difference in the highly
550 labile SOC pool (estimated by respired-C) of topsoils in deciduous and coniferous stands
551 (Fissore et al. 2008; Van Miegroet et al. 2005).

552 In our study sites, the surface layer (0–10 cm) of coniferous stands had more labile SOC
553 (lower $T_{50\_HC\_PYR}$) but also less stable SOC (lower $T_{50\_CO2\_OX}$) than in deciduous stands,
554 validating the second part of our second hypothesis. Similar findings were reported in
555 Bavarian forests, where deciduous and mixed stands showed smaller labile SOC and larger
556 stable SOC pools than coniferous stands (Wiesmeier et al. 2014).

557 Deciduous forests indeed tend to rely on a more rapid nutrient cycling between soil and plant
558 (Cole and Rapp 1981). Quideau et al. (2001) showed that oak-derived SOM has undergone
559 extensive oxidation compared with the litter, while SOM under coniferous vegetation became
560 enriched in recalcitrant alkyl C. The authors conclude that deciduous stands were
561 characterized by a high microbial activity and rapid nutrient release whereas the accumulated
562 SOM in coniferous forests had a low bioavailability. The higher pH values of the litter in
563 deciduous stands favour bioturbation and incorporation of OM in surface mineral soil,
564 whereas the more acidic coniferous litter accumulates in the organic layers (*e.g.*, Wiesmeier et

565 al. 2013). These results could also be explained by lower C/N ratios in deciduous plots (*e.g.*,
566 Cools et al. 2014). C/N ratio in deciduous stands (15.0 ± 2.8) were indeed lower than in
567 topsoils under coniferous (18.4 ± 5.1) and closer to that of the microbial biomass. This
568 difference in C/N ratios between the two vegetation types was more drastic when considering
569 the plant inputs (deciduous = 46.5 ± 9.5; coniferous = 60.9 ± 16.8; data not shown) and high
570 C/N ratios in litter are often associated with low decomposition rates (Melillo et al. 1982;
571 Norby et al. 2001; Tian et al. 2016). This would result in a higher litter mineralization
572 potential in deciduous stands and because the highly labile/labile pool is utilized more readily
573 in these plots (higher litter C turnover), it would result in a smaller size of the labile pool in
574 deciduous stands and thus a higher $T_{50\_HC\_PYR}$. Indeed, there was a negative and moderate
575 correlation between $T_{50\_HC\_PYR}$ and the inputs C/N ratio, but only in the top layer (Online
576 Resource 5). In the long term, the low C/N ratio of the deciduous litters could also explain the
577 higher $T_{50\_CO2\_OX}$ through higher SOC stabilization (Berg 2000). This highlights the
578 importance of the bulk chemistry of SOC inputs (Hobbie et al. 2007; You et al. 2016) for
579 SOC cycling. This difference in SOC stability (in the mineral soil) between the two
580 vegetation types has also been mentioned in the review by Augusto et al. (2015) and the
581 reasons of this difference identified as a future research need.
582 The limited effect of vegetation types in our study sites could be linked to species
583 heterogeneity within the two vegetation types and this might be an important limitation of this
584 work. We chose to consider vegetation types and not tree species to obtain a more balanced
585 design (29 plots in coniferous stands and 24 in deciduous stands; Fig. 1a) and our deciduous
586 stands included both beech and oak-dominated forests. Inter-species variations in terms of
587 their characteristics (*e.g.*, aboveground litter composition; roots) and their effects on the soil
588 could explain, at least partially, the limited effects of the (broad) vegetation classes in this
589 study. Some studies have indeed reported an effect of tree species on both *in-situ* and

590 laboratory soil respiration rates (measured over a year) (Hobbie et al. 2007; Vesterdal et al.
591 2012). In oak stands, the respiration rate was greater than in beech stands, but similar to those
592 in spruce stands, illustrating that the deciduous/coniferous dichotomy might be masking some
593 species effects, at least on the labile SOC pool, but quite likely also on the stable SOC pool.
594
595 d. Climatic control of the stable SOC pool
596 In our study, climate effects on SOC stability were concentrated on the stable SOC pool. Soils
597 located in plots with mountainous climate had higher C content (data not shown) than those in
598 plots in regions with oceanic or continental influence. However this higher concentration was
599 not associated with climate effects on the labile SOC indicators. Nevertheless climate was a
600 strong driver of the stable SOC indicator, SOC being less stable (lower $T_{50\_CO2\_OX}$) in
601 mountainous plots. Our last hypothesis (SOC in mountainous plots would be more labile) was
602 thus only partially verified.
603 In Bavarian forests (Wiesmeier et al. 2014), the passive SOC pool (roughly equivalent to our
604 stable SOC pool) was negatively related to MAP, which agrees with our results as the
605 mountainous plots were the wettest (1323 ± 297 mm) and there were negative correlations
606 between MAP and $T_{50\_CO2\_OX}$ in almost all layers (Online Resource 5). However, unlike us,
607 Wiesmeier et al. (2014) also detected a strong climate effect on the labile SOC as the latter
608 was under the control of both temperature and precipitation, and the most labile SOC was
609 found in mountainous regions. Similarly, Meier and Leuschner (2010) reported more labile
610 SOC when temperature decreased and precipitation increased, while Leifeld et al. (2009)
611 reported more POM-C at higher elevation in grasslands. In our study sites, there were no
612 more than weak correlations between our labile SOC pools and MAT and MAP, even when
613 considering individual layers (Online Resource 5). Nevertheless, it should be noted that the
614 mean elevation of our mountainous plots was 1230 m (± 280 m) while Leifeld et al. (2009)

had 5 out of their 8 sites located at ≥ 1410 m elevation. Finally, this "high elevation" effect on the labile fraction, expressed as POM-C requires caution as, in mountainous regions, lower MAT tend to reduce microbial activity thus favouring SOC accumulation (*e.g.,* Tewksbury and Van Miegroet 2007), even in tropical areas (Araujo et al. 2017). In cold environments, the residence time of this "labile" (as very close to the litter inputs) SOC is much longer than in more temperate climate (Leifeld et al. 2009). In that particular context, the relationship between thermal stability and SOC residence time/turnover may also be questioned and requires further study.

Another possible limitation of the present study is that vegetation and climate appeared to be confounded factors in our design with coniferous plots being preferentially found in mountainous regions: our coniferous plots had a mean elevation of 831 m (± 476 m) while it was 511 m (± 413 m) in the deciduous plots. This had an incidence on the MAT especially (Online Resource 6).

Conclusions

In this study, thanks to a large set of forest soil samples with contrasted SOC stability and the use of several indicators, we were able to highlight the influence of four environmental factors on SOC stability: depth, soil, vegetation and climate; with the degree of significance of these factors (and their interactions) varying among the SOC pools.

Our results show that pedology is a discriminant factor of SOC stability, more than individual soil physico-chemical attributes. Soil type constitutes an integrated parameter that might be an efficient way to capture SOC turnover properties. Upon modification in land management that would result in a decrease of C inputs to the soil, our results let suggest that the SOC of eutric

Cambisols may be less sensitive than the one of dystric Cambisols but specifically of entic Podzols that may be more prone to losses.

To conclude, soil class, vegetation type and climatic zone all had a significant influence on SOC stability at various depths in our studied French forest soils and these environmental factors should thus be included in models estimating the ecosystem service of climate regulation.

Acknowledgements

This work was supported by the French Environment and Energy Management Agency (ADEME) [APR REACCTIF, piCaSo project] and Campus France [PRESTIGE-2015-3-0008]. We thank M. Bryant, S. Cecchini, J. Mériguet, F. Savignac, and L. Le Vagueresse for their technical support.

References

Agnelli A, Ascher J, Corti G, Ceccherini MT, Nannipieri P, Pietramellara G (2004) Distribution of microbial communities in a forest soil profile investigated by microbial biomass, soil respiration and DGGE of total and extracellular DNA. Soil Biol Biochem. doi: 10.1016/j.soilbio.2004.02.004

Ågren GI, Hyvönen R, Berglund SL, Hobbie SE (2013) Estimating the critical N:C from litter decomposition data and its relation to soil organic matter stoichiometry. Soil Biol Biochem. doi: 10.1016/j.soilbio.2013.09.010

Amundson R (2001) The Carbon Budget in Soils. Annu Rev Earth Planet Sci 29:535-562. doi: 10.1146/annurev.earth.29.1.535

Araujo MA, Zinn YL, Lal R (2017) Soil parent material, texture and oxide contents have little effect on soil organic carbon retention in tropical highlands. Geoderma. doi: 10.1016/j.geoderma.2017.04.006

Augusto L, Ranger J, Binkley D, Rothe A (2002) Impact of several common tree species of European temperate forests on soil fertility. Ann For Sci 59:233-253

Augusto L, De Schrijver A, Vesterdal L, Smolander A, Prescott C, Ranger J (2015) Influences of evergreen gymnosperm and deciduous angiosperm tree species on the functioning of temperate and boreal forests. Biol Rev 90:444-466. doi: 10.1111/brv.12119

Balesdent J (1996) The significance of organic separates to carbon dynamics and its modelling in some cultivated soils. Eur J Soil Sci 47:485-493. doi: 10.1111/j.1365-2389.1996.tb01848.x

Barré P, Durand H, Chenu C, Meunier P, Montagne D, Castel G, Billiou D, Soucémarianadin L, Cécillon L (2017) Geological control of soil organic carbon and nitrogen stocks at the landscape scale. Geoderma 285:50-56. doi: 10.1016/j.geoderma.2016.09.029

Barré P, Plante AF, Cécillon L, Lutfalla S, Baudin F, Christensen BT, Eglin T, Fernandez JM, Houot S, Kätterer T, Le Guillou C, Macdonald A, van Oort F, Chenu C (2016) The energetic and chemical signatures of persistent soil organic matter. Biogeochemistry 130:1-12. doi: 10.1007/s10533-016-0246-0

Bates D, Mächler M, Bolker B, Walker S (2015) Fitting Linear Mixed-Effects Models Using lme4. Journal of Statistical Software, Articles 67:1-48

Bauhus J, Paré D, Côté L (1998) Effects of tree species, stand age and soil type on soil microbial biomass and its activity in a southern boreal forest. Soil Biol Biochem. doi: 10.1016/S0038-0717(97)00213-7

Behar F, Beaumont V, Penteado DB (2001) Rock-Eval 6 Technology: Performances and Developments. Oil Gas Sci Technol 56:111-134. doi: 10.2516/ogst:2001013

688 Beleites C, Sergo V (2015) hyperSpec: a package to handle hyperspectral data sets in R
689 Berg B (2000) Litter decomposition and organic matter turnover in northern forest soils.
690 For Ecol Manage 133:13-22. doi: 10.1016/S0378-1127(99)00294-7
691 Borchers HW (2015) pracma: Practical numerical math functions
692 Brêthes A, Ulrich E, Lanier M (1997) RENECOFOR : caractéristiques pédologiques des
693 102 peuplements du réseau : observations de 1994/95. Office national des forêts, Département
694 des recherches techniques, Fontainebleau, France
695 Camino-Serrano M, Gielen B, Luyssaert S, Ciais P, Vicca S, Guenet B, Vos BD, Cools N,
696 Ahrens B, Altaf Arain M, Borken W, Clarke N, Clarkson B, Cummins T, Don A, Pannatier
697 EG, Laudon H, Moore T, Nieminen TM, Nilsson MB, Peichl M, Schwendenmann L, Siemens
698 J, Janssens I (2014) Linking variability in soil solution dissolved organic carbon to climate,
699 soil type, and vegetation type. Glob Biogeochem Cycles 28:497-509. doi:
700 10.1002/2013GB004726
701 Canadell JG, Le Quéré C, Raupach MR, Field CB, Buitenhuis ET, Ciais P, Conway TJ,
702 Gillett NP, Houghton RA, Marland G (2007) Contributions to accelerating atmospheric CO_2
703 growth from economic activity, carbon intensity, and efficiency of natural sinks. PNAS
704 104:18866-18870. doi: 10.1073/pnas.0702737104
705 Cardinael R, Chevallier T, Barthès BG, Saby NPA, Parent T, Dupraz C, Bernoux M,
706 Chenu C (2015) Impact of alley cropping agroforestry on stocks, forms and spatial
707 distribution of soil organic carbon — A case study in a Mediterranean context. Geoderma
708 259–260:288-299. doi: 10.1016/j.geoderma.2015.06.015
709 Carter MR, Gregorich EG, Angers DA, Donald RG, Bolinder MA (1998) Organic C and N
710 storage, and organic C fractions, in adjacent cultivated and forested soils of eastern Canada.
711 Soil Tillage Res. doi: 10.1016/S0167-1987(98)00114-7

712 Cécillon L, Baudin F, Chenu C, Houot S, Jolivet R, Kätterer T, Lutfalla S, Macdonald A,
713 van Oort F, Plante AF, Savignac F, Soucémarianadin L, Barré P (2018) A model based on
714 Rock-Eval thermal analysis to quantify the size of the centennially persistent organic carbon
715 pool in temperate soils. Biogeosciences Discussions 2018:1-25. doi: 10.5194/bg-2018-15
716 Cleveland CC, Liptzin D (2007) C:N:P stoichiometry in soil: is there a "Redfield ratio" for
717 the microbial biomass?. Biogeochemistry 85:235-252. doi: 10.1007/s10533-007-9132-0
718 Cole DW, Rapp M (1981) Elemental cycling in forest ecosystems. In: Reichle DE (ed)
719 Dynamic Properties of Forest Ecosystems. Cambridge University Press, pp 341-409
720 Coleman K, Jenkinson D (1999) RothC-26.3. A Model for the Turn-over of Carbon in
721 Soils. Model Description and Windows Users Guide. IACR – Rothamsted, Harpenden.
722 Cools N, Vesterdal L, De Vos B, Vanguelova E, Hansen K (2014) Tree species is the
723 major factor explaining C:N ratios in European forest soils. Forest Ecol Manag. doi:
724 10.1016/j.foreco.2013.06.047
725 Cotrufo FM, Ineson P, Roberts DJ (1995) Decomposition of birch leaf litters with varying
726 C-to-N ratios. Soil Biol Biochem. doi: 10.1016/0038-0717(95)00043-E "
727 Crow SE, Swanston CW, Lajtha K, Brooks JR, Keirstead H (2007) Density fractionation
728 of forest soils: methodological questions and interpretation of incubation results and turnover
729 time in an ecosystem context. Biogeochemistry 85:69-90. doi: 10.1007/s10533-007-9100-8
730 Curtin D, Campbell CA, Jalil A (1998) Effects of acidity on mineralization: pH-
731 dependence of organic matter mineralization in weakly acidic soils. Soil Biol Biochem. doi:
732 10.1016/S0038-0717(97)00094-1
733 Diochon AC, Kellman L (2009) Physical fractionation of soil organic matter:
734 Destabilization of deep soil carbon following harvesting of a temperate coniferous forest. J
735 Geophys Res 114. doi: 10.1029/2008JG000844

Disnar JR, Guillet B, Keravis D, Di-Giovanni C, Sebag D (2003) Soil organic matter (SOM) characterization by Rock-Eval pyrolysis: scope and limitations. Org Geochem 34:327-343. doi: 10.1016/S0146-6380(02)00239-5

Dodla SK, Wang JJ, DeLaune RD (2012) Characterization of labile organic carbon in coastal wetland soils of the Mississippi River deltaic plain: Relationships to carbon functionalities. Sci Total Environ 435–436:151-158. doi: 10.1016/j.scitotenv.2012.06.090

Dungait JAJ, Hopkins DW, Gregory AS, Whitmore AP (2012) Soil organic matter turnover is governed by accessibility not recalcitrance. Glob Change Biol 18:1781-1796. doi: 10.1111/j.1365-2486.2012.02665.x

Feng W, Shi Z, Jiang J, Xia J, Liang J, Zhou J, Luo Y (2016) Methodological uncertainty in estimating carbon turnover times of soil fractions. Soil Biol Biochem 100:118-124. doi: 10.1016/j.soilbio.2016.06.003

Fissore C, Giardina CP, Kolka RK, Trettin CC, King GM, Jurgensen MF, Barton CD, McDowell SD (2008) Temperature and vegetation effects on soil organic carbon quality along a forested mean annual temperature gradient in North America. Global Change Biol 14:193-205. doi: 10.1111/j.1365-2486.2007.01478.x

Fox J, Weisberg S (2011) An R Companion to Applied Regression

Frøseth RB, Bleken MA (2015) Effect of low temperature and soil type on the decomposition rate of soil organic carbon and clover leaves, and related priming effect. Soil Biol Biochem. doi: 10.1016/j.soilbio.2014.10.004

Gillespie AW, Sanei H, Diochon A, Ellert BH, Regier TZ, Chevrier D, Dynes JJ, Tarnocai C, Gregorich EG (2014) Perennially and annually frozen soil carbon differ in their susceptibility to decomposition: Analysis of Subarctic earth hummocks by bioassay, XANES and pyrolysis. Soil Biol Biochem 68:106-116. doi: 10.1016/j.soilbio.2013.09.021

760 Golchin A, Oades JM, Skjemstad JO, Clarke P (1994) Study of free and occluded
761 particulate organic matter in soils by solid state ^{13}C CP/MAS NMR spectroscopy and
762 scanning electron microscopy. Aust J Soil Res 32:285-309. doi: 10.1071/SR9940285
763 Gregorich EG, Gillespie AW, Beare MH, Curtin D, Sanei H, Yanni SF (2015) Evaluating
764 biodegradability of soil organic matter by its thermal stability and chemical composition. Soil
765 Biol Biochem 91:182-191. doi: 10.1016/j.soilbio.2015.08.032
766 Harris D, Horwáth WR, van Kessel C (2001) Acid fumigation of soils to remove
767 carbonates prior to total organic carbon or CARBON-13 isotopic analysis. Soil Sci Soc Am J
768 65:1853-1856. doi: 10.2136/sssaj2001.1853
769 Hassink J (1995) Density fractions of soil macroorganic matter and microbial biomass as
770 predictors of C and N mineralization. Soil Biol Biochem 27:1099-1108. doi: 10.1016/0038-
771 0717(95)00027-C
772 Hobbie SE, Ogdahl M, Chorover J, Chadwick OA, Oleksyn J, Zytkowiak R, Reich PB
773 (2007) Tree species effects on soil organic matter dynamics: The role of soil cation
774 composition. Ecosystems 10:999-1018. doi: 10.1007/s10021-007-9073-4
775 Intergovernmental Panel on Climate Change (2000) Land Use, Land-Use Change and
776 Forestry - A Special Report of the IPCC. Cambridge University Press, Cambridge, UK
777 IUSS Working Group (2015) World reference base for soil resources 2014 (update 2015),
778 international soil classification system for naming soils and creating legends for soil maps.
779 World Soil Resources Reports
780 Jandl R, Lindner M, Vesterdal L, Bauwens B, Baritz R, Hagedorn F, Johnson DW,
781 Minkkinen K, Byrne KA (2007) How strongly can forest management influence soil carbon
782 sequestration?. Geoderma 137:253-268. doi: 10.1016/j.geoderma.2006.09.003

783 Jarvis PG, Ibrom A, Linder S (2005) 'Carbon forestry': managing forests to conserve
784 carbon. In: Griffiths HG, Jarvis PG (eds) The Carbon Balance of Forest Biomes. Taylor &
785 Francis, pp 356-377
786 Jenkinson DS, Poulton PR, Bryant C (2008) The turnover of organic carbon in subsoils.
787 Part 1. Natural and bomb radiocarbon in soil profiles from the Rothamsted long-term field
788 experiments. Eur J Soil Sci 59:391-399. doi: 10.1111/j.1365-2389.2008.01025.x
789 Jobbágy EG, Jackson RB (2000) The vertical distribution of soil organic carbon and its
790 relation to climate and vegetation. Ecol Appl 10:423-436. doi: 10.1890/1051-
791 0761(2000)010[0423:TVDOSO]2.0.CO;2
792 Jonard M, Nicolas M, Coomes DA, Caignet I, Saenger A, Ponette Q (2017) Forest soils in
793 France are sequestering substantial amounts of carbon. Sci Total Environ 574:616-628. doi:
794 10.1016/j.scitotenv.2016.09.028
795 Kassambara A, Mundt F (2016) factoextra: Extract and Visualize the Results of
796 Multivariate Data Analyses
797 Kindermann G, McCallum I, Fritz S, Obersteiner M (2008) A global forest growing stock,
798 biomass and carbon map based on FAO statistics. Silva Fenn 42. doi: 10.14214/sf.244
799 Lafargue E, Marquis F, Pillot D (1998) Rock-Eval 6 Applications in Hydrocarbon
800 Exploration, Production, and Soil Contamination Studies. Oil Gas Sci Technol 53:421-437.
801 doi: 10.2516/ogst:1998036
802 Laganière J, Paré D, Bergeron Y, Chen HYH (2012) The effect of boreal forest
803 composition on soil respiration is mediated through variations in soil temperature and C
804 quality. Soil Biol Biochem. doi: 10.1016/j.soilbio.2012.04.024
805 Leifeld J, Zimmerman M, Fuhrer J, Conen F (2009) Storage and turnover of carbon in
806 grassland soils along an elevation gradient in the Swiss Alps. Global Change Biol 15:668-
807 679. doi: 10.1111/j.1365-2486.2008.01782.x

Lorenz K, Lal R (2010) Carbon Sequestration in Forest Ecosystems. Springer Netherlands

Lorenz K, Lal R (2005) The depth distribution of soil organic carbon in relation to land use and management and the potential of carbon sequestration in subsoil horizons. Adv Agron 88:35-66. doi: 10.1016/S0065-2113(05)88002-2

Mason JA, Jacobs PM, Gruley KE, Reyerson P, Hanson PR (2016) Parent material influence on soil response to vegetation change, Southeastern Minnesota, U.S.A. Geoderma 275:1-17. doi: 10.1016/j.geoderma.2016.04.004

Mathieu JA, Hatté C, Balesdent J, Parent É (2015) Deep soil carbon dynamics are driven more by soil type than by climate: a worldwide meta-analysis of radiocarbon profiles. Global Change Biol 21:4278-4292. doi: 10.1111/gcb.13012

Meier IC, Leuschner C (2010) Variation of soil and biomass carbon pools in beech forests across a precipitation gradient. Global Change Biol 16:1035-1045. doi: 10.1111/j.1365-2486.2009.02074.x

Melillo JM, Aber JD, Muratore JF (1982) Nitrogen and lignin control of hardwood leaf litter decomposition dynamics. Ecology 63:621-626. doi: 10.2307/1936780

Moni C, Rumpel C, Virto I, Chabbi A, Chenu C (2010) Relative importance of sorption versus aggregation for organic matter storage in subsoil horizons of two contrasting soils. Eur J Soil Sci 61:958-969. doi: 10.1111/j.1365-2389.2010.01307.x

Mulder VL, Lacoste M, Martin MP, Richer-de-Forges A, Arrouays D (2015) Understanding large-extent controls of soil organic carbon storage in relation to soil depth and soil-landscape systems. Glob Biogeochem Cycles 29:1210-1229. doi: 10.1002/2015GB005178

Nabuurs GJ, Thürig E, Heidema N, Armolaitis K, Biber P, Cienciala E, Kaufmann E, Mäkipää R, Nilsen P, Petritsch R, Pristova T, Rock J, Schelhaas MJ, Sievanen R, Somogyi Z,

832 Vallet P (2008) Hotspots of the European forests carbon cycle. For Ecol Manag. doi:
833 10.1016/j.foreco.2008.04.009
834 Norby RJ, Cotrufo MF, Ineson P, O'Neill EG, Canadell JG (2001) Elevated CO_2, litter
835 chemistry, and decomposition: a synthesis. Oecologia 127:153-165. doi:
836 10.1007/s004420000615
837 Olsen HR, Van Miegroet H (2010) Factors affecting carbon dioxide release from forest and
838 rangeland soils in Northern Utah. Soil Sci Soc Am J 74:282-291. doi: 10.2136/sssaj2009.0095
839 Pan Y, Birdsey RA, Fang J, Houghton RA, Kauppi PE, Kurz WA, Phillips OL, Shvidenko
840 AZ, Lewis SL, Canadell JG, Ciais P, Jackson RB, Pacala SW, McGuire AD, Piao S,
841 Rautiainen A, Sitch S, Hayes D (2011) A large and persistent carbon sink in the world's
842 forests. Science 333:988-993. doi: 10.1126/science.1201609
843 Pinheiro J, Bates D, DebRoy S, Sarkar D, Team RC (2016) nlme: Linear and Nonlinear
844 Mixed Effects Models
845 Plante AF, Fernández JM, Leifeld J (2009) Application of thermal analysis techniques in
846 soil science. Geoderma 153:1-10. doi: 10.1016/j.geoderma.2009.08.016
847 Poeplau C, Don A (2013) Sensitivity of soil organic carbon stocks and fractions to
848 different land-use changes across Europe. Geoderma. doi: 10.1016/j.geoderma.2012.08.003
849 Ponette Q, Ulrich E, Brêthes A, Bonneau M, Lanier M (1997) RENECOFOR - Chimie des
850 sols dans les 102 peuplements du réseau : campagne de mesures 1993-95. ONF, Département
851 des recherches techniques, Fontainebleau, France
852 Prescott CE (2010) Litter decomposition: what controls it and how can we alter it to
853 sequester more carbon in forest soils? Biogeochemistry 101:133-149. doi: 10.1007/s10533-
854 010-9439-0

Quideau SA, Chadwick OA, Benesi A, Graham RC, Anderson MA (2001) A direct link between forest vegetation type and soil organic matter composition. Geoderma. doi: 10.1016/S0016-7061(01)00055-6

R Core Team (2016) R: A Language and Environment for Statistical Computing

Rowley MC, Grand S, Verrecchia EP (2018) Calcium-mediated stabilisation of soil organic carbon. Biogeochemistry 137:27-49. doi: 10.1007/s10533-017-0410-1

Rumpel C, Kögel-Knabner I (2010) Deep soil organic matter---a key but poorly understood component of terrestrial C cycle. Plant Soil 338:143-158. doi: 10.1007/s11104-010-0391-5

Saenger A, Cécillon L, Poulenard J, Bureau F, De Daniéli S, Gonzalez J, Brun J (2015) Surveying the carbon pools of mountain soils: A comparison of physical fractionation and Rock-Eval pyrolysis. Geoderma 241–242:279-288. doi: 10.1016/j.geoderma.2014.12.001

Salomé C, Nunan N, Pouteau V, Lerch TZ, Chenu C (2010) Carbon dynamics in topsoil and in subsoil may be controlled by different regulatory mechanisms. Global Change Biol 16:416-426. doi: 10.1111/j.1365-2486.2009.01884.x

Schiedung M, Don A, Wordell-Dietrich P, Alcántara V, Kuner P, Guggenberger G (2017) Thermal oxidation does not fractionate soil organic carbon with differing biological stabilities. J Plant Nutr Soil Sci 180:18-26. doi: 10.1002/jpln.201600172

Schmatz R, Recous S, Aita C, Tahir MM, Schu AL, Chaves B, Giacomini SJ (2017) Crop residue quality and soil type influence the priming effect but not the fate of crop residue C. Plant Soil 414:229-245. doi: 10.1007/s11104-016-3120-x

Schmidt MWI, Torn MS, Abiven S, Dittmar T, Guggenberger G, Janssens IA, Kleber M, Kögel-Knabner I, Lehmann J, Manning DAC, Nannipieri P, Rasse DP, Weiner S, Trumbore SE (2011) Persistence of soil organic matter as an ecosystem property. Nature 478:49-56. doi: 10.1038/nature10386

880 Schrumpf M, Kaiser K, Guggenberger G, Persson T, Kögel-Knabner I, Schulze E- (2013)
881 Storage and stability of organic carbon in soils as related to depth, occlusion within
882 aggregates, and attachment to minerals. Biogeosciences 10:1675-1691. doi: 10.5194/bg-10-
883 1675-2013
884 Schrumpf M, Kaiser K (2015) Large differences in estimates of soil organic carbon
885 turnover in density fractions by using single and repeated radiocarbon inventories. Geoderma
886 239–240:168-178. doi: 10.1016/j.geoderma.2014.09.025
887 Sebag D, Verrecchia EP, Cécillon L, Adatte T, Albrecht R, Aubert M, Bureau F, Cailleau
888 G, Copard Y, Decaens T, Disnar J-, Hetényi M, Nyilas T, Trombino L (2016) Dynamics of
889 soil organic matter based on new Rock-Eval indices. Geoderma 284:185-203. doi:
890 10.1016/j.geoderma.2016.08.025
891 Six J, Conant RT, Paul EA, Paustian K (2002) Stabilization mechanisms of soil organic
892 matter: Implications for C-saturation of soils. Plant Soil 241:155-176. doi:
893 10.1023/A:1016125726789
894 Sjögersten S, Alewell C, Cécillon L, Hagedorn F, Jandl R, Leifeld J, Martinsen V,
895 Schindlbacher A, Sebastià M-, Van Miegroet H (2011) Mountain Soils in a Changing
896 Climate? Vulnerability of Carbon Stocks and Ecosystem Feedbacks. In: Soil Carbon in
897 Sensitive European Ecosystems. John Wiley & Sons, Ltd, Chichester, UK, pp 118-148
898 Smith P, Bustamante M, Ahammad H, Clark H, Dong H, Elsiddig EA, Haberl H, Harper
899 R, House J, Jafari M, Masera O, Mbow C, Ravindranath NH, Rice CW, Robledo Abad C,
900 Romanovskaya A, Sperling F, Tubiello F (2014) Agriculture, Forestry and Other Land Use
901 (AFOLU). In: Edenhofer O, Pichs-Madruga R, Sokona Y, Farahani E, Kadner S, Seyboth K,
902 Adler A, Baum I, Brunner S, Eickemeier P, Kriemann B, Savolainen J, Schlömer S, von
903 Stechow C, Zwickel T, Minx JC (eds) Climate Change 2014: Mitigation of Climate Change.
904 Contribution of Working Group III to the Fifth Assessment Report of the Intergovernmental

905 Panel on Climate Change. Cambridge University Press, Cambridge, UK and New York, NY,
906 USA, pp 811-922
907 Soucémarianadin LN, Cécillon L, Chenu C, Baudin F, Nicolas M, Girardin C, Barré P
908 (2018) Is Rock-Eval 6 thermal analysis a good indicator of soil organic carbon lability? - A
909 method-comparison study in forest soils. Soil Biol Biochem 117:108-116. doi:
910 10.1016/j.soilbio.2017.10.025
911 Tewksbury CE, Van Miegroet H (2007) Soil organic carbon dynamics along a climatic
912 gradient in a southern Appalachian spruce–fir forest. Can J For Res 37:1161-1172. doi:
913 10.1139/X06-317
914 Tian Q, He H, Cheng W, Bai Z, Wang Y, Zhang X (2016) Factors controlling soil organic
915 carbon stability along a temperate forest altitudinal gradient. Sci Rep 6:18783. doi:
916 10.1038/srep18783
917 Torn MS, Trumbore SE, Chadwick OA, Vitousek PM, Hendricks DM (1997) Mineral
918 control of soil organic carbon storage and turnover. Nature 389:170-173. doi: 10.1038/38260
919 Trumbore SE (1997) Potential responses of soil organic carbon to global environmental
920 change. Proc Natl Acad Sci U S A 94:8284-8291
921 Trumbore SE, Chadwick OA, Amundson R (1996) Rapid exchange between soil carbon
922 and atmospheric carbon dioxide driven by temperature change. Science. doi:
923 10.1126/science.272.5260.393
924 Tyrrell ML, Ross J, Kelty M (2012) Carbon Dynamics in the Temperate Forest. In: Ashton
925 MS, Tyrrell ML, Spalding D, Gentry B (eds) Managing Forest Carbon in a Changing Climate.
926 Springer Netherlands, Dordrecht, pp 77-107
927 Ulrich E (1995) Le réseau RENECOFOR : objectifs et réalisation. Rev for fr 47:107-124.
928 doi: 10.4267/2042/26634

Van Miegroet H, Boettinger JL, Baker MA, Nielsen J, Evans D, Stum A (2005) Soil carbon distribution and quality in a montane rangeland-forest mosaic in northern Utah. Forest Ecol Manag. doi: 10.1016/j.foreco.2005.08.017

Vesterdal L, Elberling B, Christiansen JR, Callesen I, Schmidt IK (2012) Soil respiration and rates of soil carbon turnover differ among six common European tree species. For Ecol Manag 264:185-196. doi: 10.1016/j.foreco.2011.10.009

von Lützow M, Kögel-Knabner I, Ekschmitt K, Flessa H, Guggenberger G, Matzner E, Marschner B (2007) SOM fractionation methods: Relevance to functional pools and to stabilization mechanisms. Soil Biol Biochem 39:2183-2207. doi: 10.1016/j.soilbio.2007.03.007

Vos C, Jaconi A, Jacobs A, Don A (2017) Hot regions of labile and stable soil organic carbon in Germany -- Spatial variability and driving factors. SOIL 2017:1-35. doi: 10.5194/soil-2017-30

Wander M (2004) Soil organic matter fractions and their relevance to soil function. In: Magdoff F, Weil RR (eds) Soil Organic Matter in Sustainable Agriculture. CRC Press, pp 67-102

Wang Q, Zhong M (2016) Composition and mineralization of soil organic carbon pools in four single-tree species forest soils. Journal of Forestry Research 27:1277-1285. doi: 10.1007/s11676-016-0244-z

Wiesmeier M, Prietzel J, Barthold F, Spörlein P, Geuß U, Hangen E, Reischl A, Schilling B, von Lützow M, Kögel-Knabner I (2013) Storage and drivers of organic carbon in forest soils of southeast Germany (Bavaria) – Implications for carbon sequestration. For Ecol Manag 295:162-172. doi: 10.1016/j.foreco.2013.01.025

Wiesmeier M, Schad P, von Lützow M, Poeplau C, Spörlein P, Geuß U, Hangen E, Reischl A, Schilling B, Kögel-Knabner I (2014) Quantification of functional soil organic carbon pools

954 for major soil units and land uses in southeast Germany (Bavaria). Agric Ecosyst Environ.
955 doi: 10.1016/j.agee.2013.12.028
956 Wordell-Dietrich P, Don A, Helfrich M (2017) Controlling factors for the stability of
957 subsoil carbon in a Dystric Cambisol. Geoderma. doi: 10.1016/j.geoderma.2016.08.023
958 You Y, Wang J, Sun X, Tang Z, Zhou Z, Sun OJ (2016) Differential controls on soil
959 carbon density and mineralization among contrasting forest types in a temperate forest
960 ecosystem. Sci Rep 6:22411. doi: 10.1038/srep22411
961 Zhang J, Song C, Wenyan Y (2007) Tillage effects on soil carbon fractions in the Sanjiang
962 Plain, Northeast China. Soil Tillage Res. doi: 10.1016/j.still.2006.03.014
963 Zimmermann M, Leifeld J, Schmidt MWI, Smith P, Fuhrer J (2007) Measured soil organic
964 matter fractions can be related to pools in the RothC model. Eur J Soil Sci 58:658-667. doi:
965 10.1111/j.1365-2389.2006.00855.x
966

Figures captions

Fig. 1 (a) Location of the 53 study sites from the French national network for the long term monitoring of forest ecosystems (RENECOFOR) and their repartition among the climatic zones and vegetation types and soil classes; (b) Number of samples by depths and analyses performed to assess SOC stability

Fig. 2 Evolution of respired-C, POM-C, $T_{50\_HC\_PYR}$ and $T_{50\_CO2\_OX}$ in the five soil layers of the 53 RENECOFOR plots. The horizontal black lines show the medians. The bottom and top of the box show the first and third quartiles, respectively. n= 53 for layers 0–10 cm, 10–20 cm and 20–40 cm; n = 50 (RE6 and POM-C) or 46 (respired-C) for layer 40–80 cm; n = 33 (RE6) or 31 (respired-C) for layer 80–100 cm. For each indicator, different letters indicate significant differences between the means of the different layers

Fig. 3 Variations in the indicators of SOC stability respired-C and POM-C (top) and thermal indicators ($T_{50\_HC\_PYR}$ and $T_{50\_CO2\_OX}$; bottom) as a function of vegetation type in the surface (0–10 cm) layer. The horizontal black line shows the median for each vegetation type. The bottom and top of the box show the first and third quartiles, respectively. n = 29 and 24 for coniferous and deciduous plots respectively. For each indicator, different letters indicate significant differences between the means of the different layers

Fig. 4 Variations in indicators of SOC stability respired-C and POM-C (top) and thermal indicators ($T_{50\_HC\_PYR}$ and $T_{50\_CO2\_OX}$; bottom) as a function of depth for all three soil classes. n= 53 for layers 0–10 cm, 10–20 cm and 20–40 cm; n = 50 (RE6 and POM-C) or 46 (respired-C) for layer 40–80 cm; n = 33 (RE6) or 31 (respired-C) for layer 80–100 cm

Fig. 5 Variations in the thermal indicator $T_{50\_CO2\_OX}$ (stable SOC pool) in the three climatic zones as a function of depth

Fig. 6 Principal components analysis (PCA) loadings plots (top) and biplots (bottom) of the 4 indicators of SOC stability (red arrows) along the first two principal component axes (PC1 and PC2) for two layers: (left) 0–10 cm (n = 53) and (right) 40–80 cm (n = 46). In the loading plots, the physico-chemical parameters and climatic data (black arrows) were projected in the circle of correlations for information. In the biplots, the samples were represented by their soil class and the 95% ellipses for the three soil classes were added

Table 1 Mean (and standard deviation) of SOC content, C/N ratio of the bulk soil and RE6-derived bulk chemistry parameters (HI, OI_{RE6}), as well as the averaged values derived from Ponette et al. (1997) and Jonard et al. (2017) for the texture, pH_{water} and the cationic exchange capacity, in the five soil layers for the 53 RENECOFOR plots

depth (cm)	n	SOC		C/N ratio		HI		OI_{RE6}		clay		silt		sand		pH_{water}		CEC[a]	
		%				mg HC / g SOC)		mg O_2 / g SOC		%		%		%				cmol+/kg	
		(composite sample, determined in this study)								(averaged from Ponette et al., 1997 and Jonard et al. 2017)									
0–10	53	5.1	(2.7)	16.9	(4.5)	276	(77)	225	(37)	23	(14)	36	(18)	42	(29)	4.9	(1.0)	13.3	(13.1)
10–20	53	2.9	(2.0)	16.4	(4.9)	218	(72)	255	(46)	21	(13)	37	(18)	42	(29)	5.1	(1.1)	10.9	(12.7)
20–40	53	1.8	(1.4)	14.8	(4.3)	170	(57)	299	(68)	20	(14)	36	(18)	43	(28)	5.4	(1.3)	10.0	(12.5)
40–80	50	0.8	(0.8)	11.6	(3.8)	133	(33)	437	(137)	20	(15)	32	(17)	48	(27)	5.8	(1.4)	7.3	(8.5)
80–100	33	0.6	(0.5)	9.7	(4.0)	122	(27)	525	(145)	22	(17)	34	(16)	44	(27)	6.1	(1.6)	7.5	(8.3)

[a] determined by extraction of the exchangeable cations with barium chloride (ISO 11260:1994)

Table 2 Results (*p*-value) of the 3-way ANOVA (analysis by layer) with the factors soil class (soil), vegetation type (veg) and climatic zone (clim) and their interactions for each response variable obtained from respiration test (respired-C), POM fractionation (POM-C) and RE6 thermal analysis ($T_{50\_HC\_PYR}$; $T_{50\_CO2\_OX}$). If the response variable needed to be transformed to conform to the assumptions of ANOVA, the transformation that was used is specified. Significance is indicated as follows: ***: $p < 0.001$; **: $p < 0.01$; *: $p < 0.05$; .: $p < 0.1$; NS = not significant

		Factor			Interaction		
Respiration test							
depth (cm)	variable	soil	veg	clim	soil × veg	soil × clim	veg × clim
0–10	respired-C	**	NS	NS	NS	NS	NS
10–20	$\log_{10}$ (respired-C + 1)	***	NS	NS	NS	NS	NS
20–40	$\log_{10}$ (respired-C + 1)	**	NS	NS	NS	NS	NS
40–80	$\log_{10}$ (respired-C + 1)	NS	NS	NS	NS	NS	NS
80–100	$\log_{10}$ (respired-C + 1)	*	NS	NS	NS	NS	NS
POM fractionation							
depth (cm)	variable	soil	veg	clim	soil × veg	soil × clim	veg × clim
0–10	POM-C	*	NS	NS	NS	NS	NS
40–80	POM-C	*	NS	NS	NS	NS	NS
Rock-Eval thermal analysis							
depth (cm)	variable	soil	veg	clim	soil × veg	soil × clim	veg × clim
0–10	$T_{50\_HC\_PYR}$	***	***	NS	NS	.	NS
10–20	$T_{50\_HC\_PYR}$	NS	NS	NS	.	NS	NS
20–40	$T_{50\_HC\_PYR}$	*	NS	NS	NS	NS	NS
40–80	$T_{50\_HC\_PYR}$	NS	NS	NS	NS	NS	NS
80–100	$T_{50\_HC\_PYR}$	NS	NS	NS	NS	NS	NS
0–10	$T_{50\_CO2\_OX}$	**	***	**	NS	NS	NS
10–20	$T_{50\_CO2\_OX}$	NS	*	**	NS	*	NS
20–40	$T_{50\_CO2\_OX}$	NS	*	**	NS	*	NS
40–80	$T_{50\_CO2\_OX}$	*	NS	***	NS	NS	NS
80–100	$T_{50\_CO2\_OX}$	NS	NS	*	NS	NS	NS

Table 3 Spearman correlation coefficients between the RE6-derived temperature parameters ($T_{50\_HC\_PYR}$ and $T_{50\_CO2\_OX}$), the 10-week mineralizable SOC (respired-C), the proportion of SOC in the POM fraction (POM-C) and the physico-chemical properties of the samples (C content; C/N ratio; HI; OI_{RE6}; texture, clay and sand content; pH; cationic exchange capacity, CEC) and climatic data of the plots (mean annual precipitation, MAP; mean annual temperature, MAT). Significance is indicated as follows: ***: $p < 0.001$; **: $p < 0.01$; *: $p < 0.05$. The high (> 0.6) correlations are marked in bold. n = 242 for the RE6 parameters, n = 236 for respired-C and n = 103 for POM-C

	$T_{50\_HC\_PYR}$	$T_{50\_CO2\_OX}$	respired-C	POM-C
SOC	−0.58***	**−0.72***	0.03	0.52***
C/N ratio	−0.34***	−0.43***	−0.13*	**0.61***
HI	**−0.67***	−0.53***	0.08	**0.67****
OI_{RE6}	**0.63****	0.50***	−0.04	**−0.76****
Clay	−0.06	−0.03	0.19**	−0.18
Sand	0.02	0.10	−0.15*	0.18
pH_{water}	0.31***	0.33***	0.23***	−0.54***
CEC	−0.33***	−0.25***	0.31***	0.08
MAP	0.06	−0.20**	−0.16*	−0.11
MAT	0.01	0.19**	−0.09	−0.02

Fig. 1

Click here to download colour figure Fig1.tif

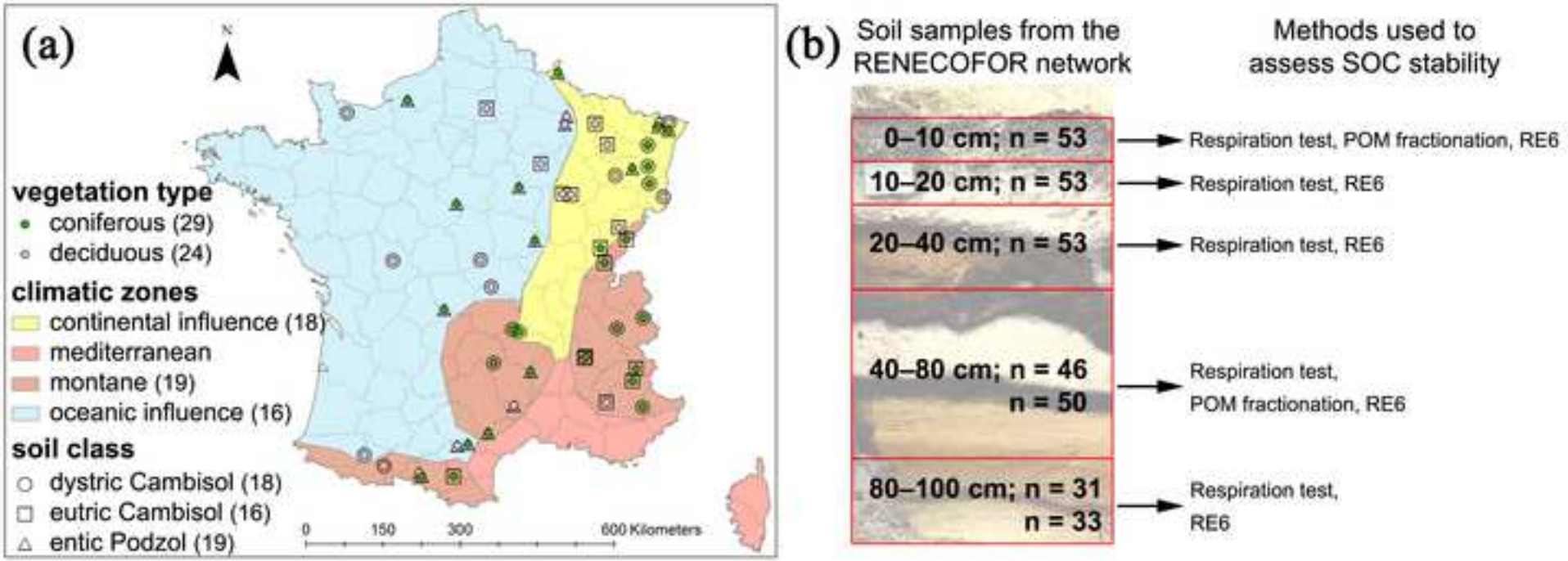

Fig. 2

Click here to download colour figure Fig2.tif

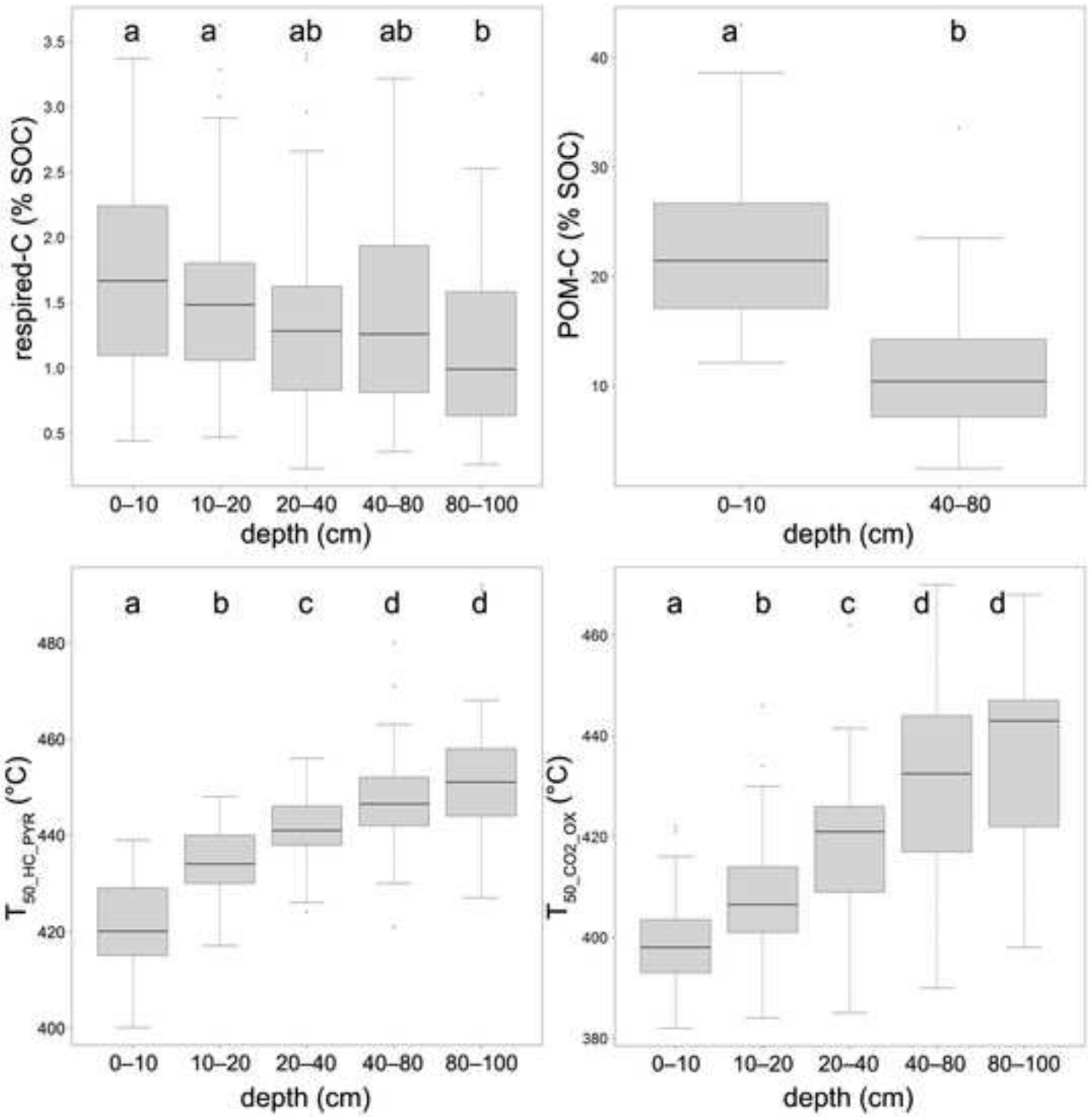

Fig. 3

Click here to download colour figure Fig3.tif

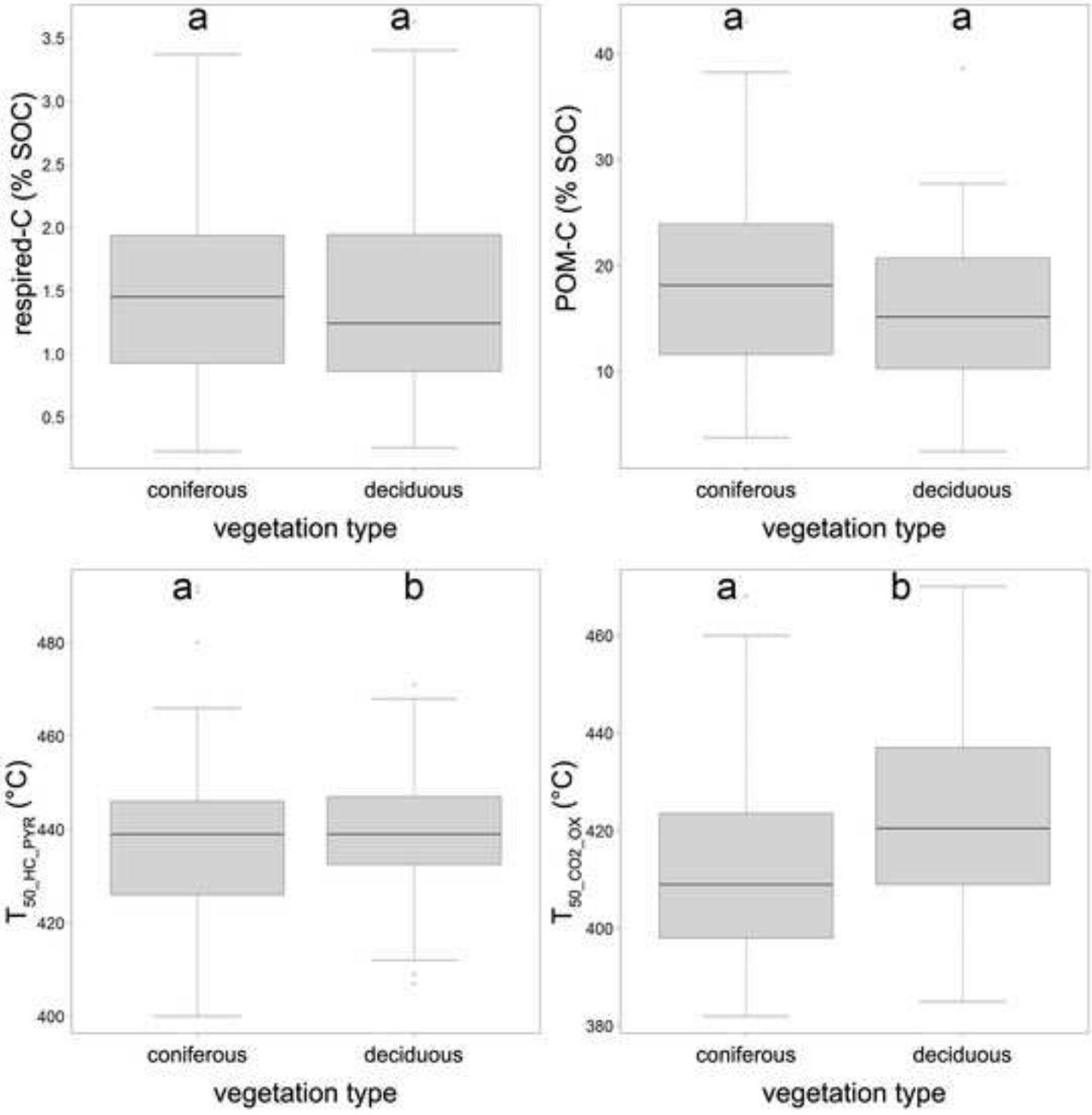

Fig. 4

Click here to download colour figure Fig4.tif

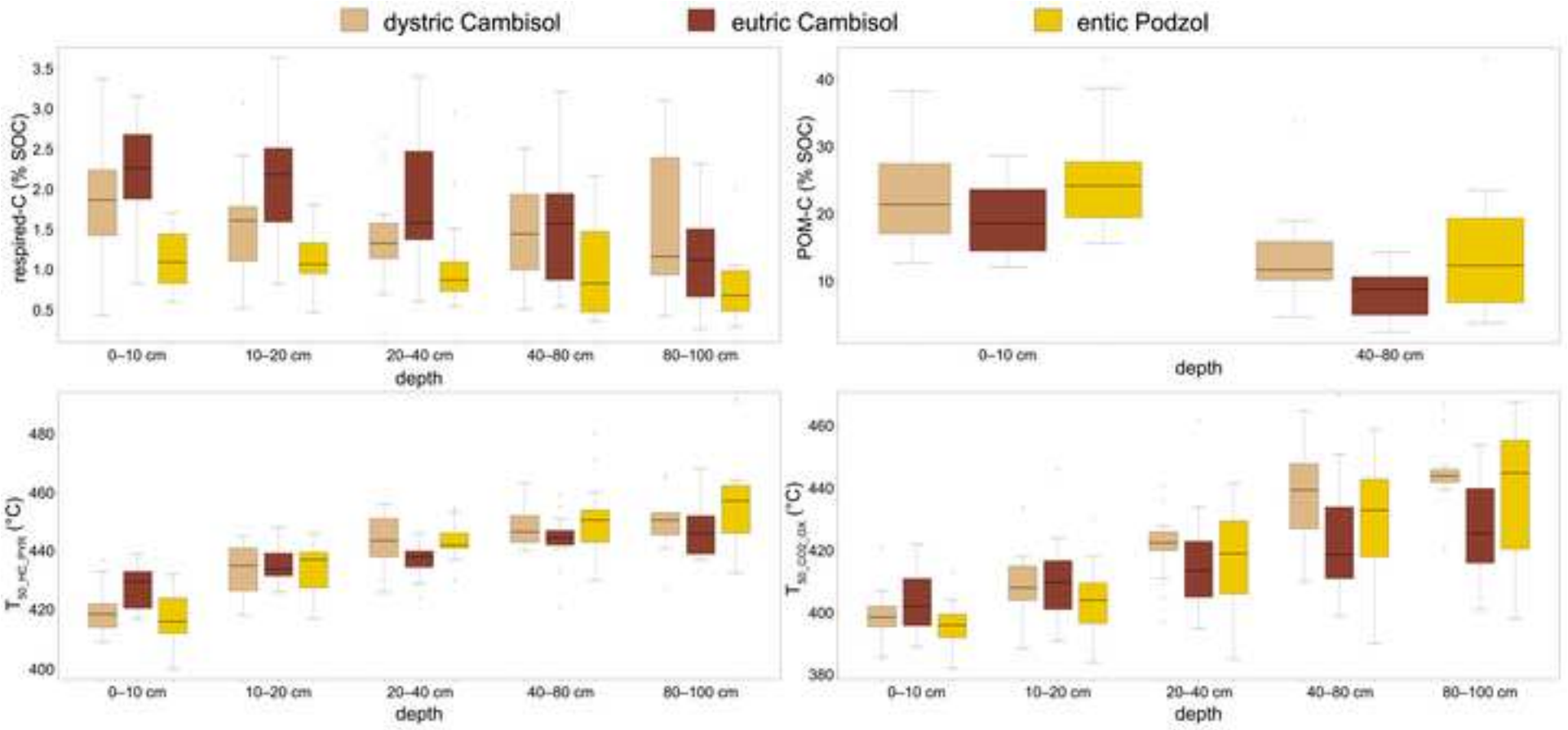

Fig. 5

Click here to download colour figure Fig5.tif

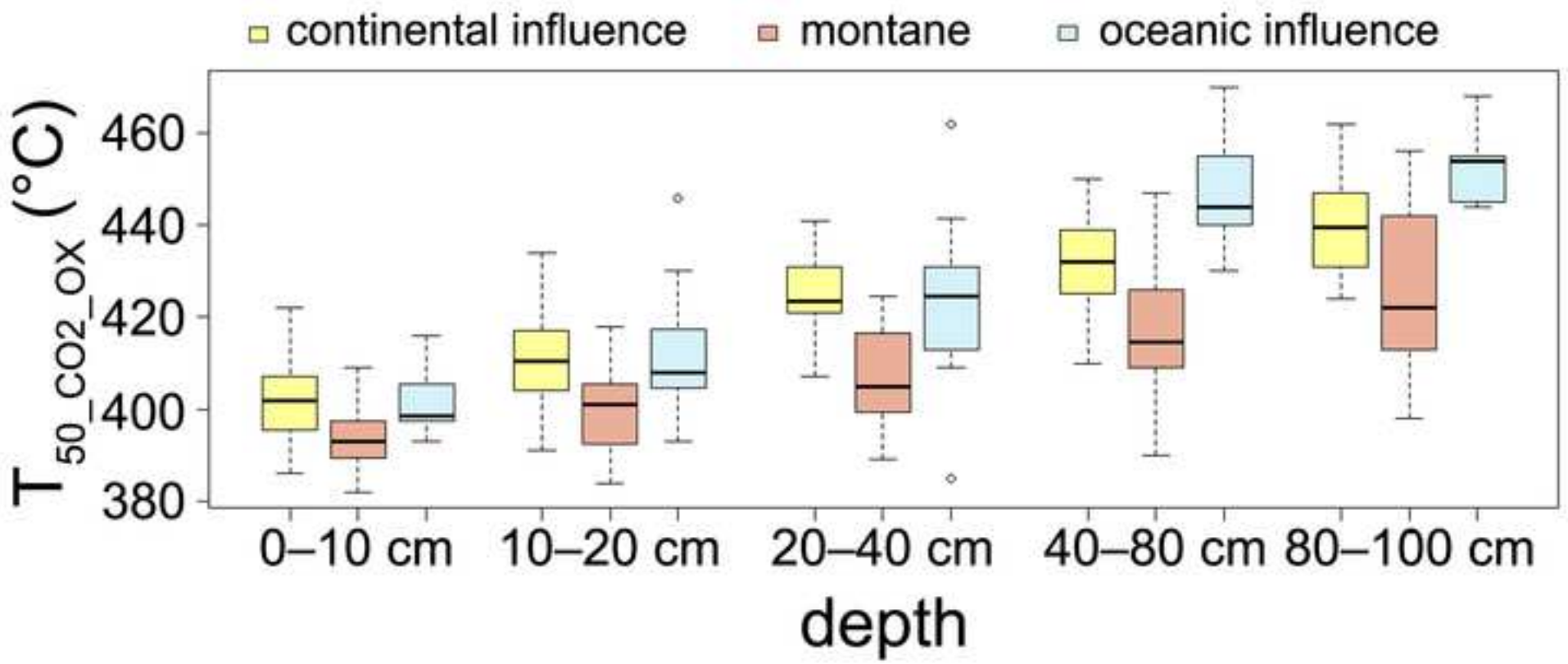

Fig. 6

Click here to download colour figure Fig6.tif

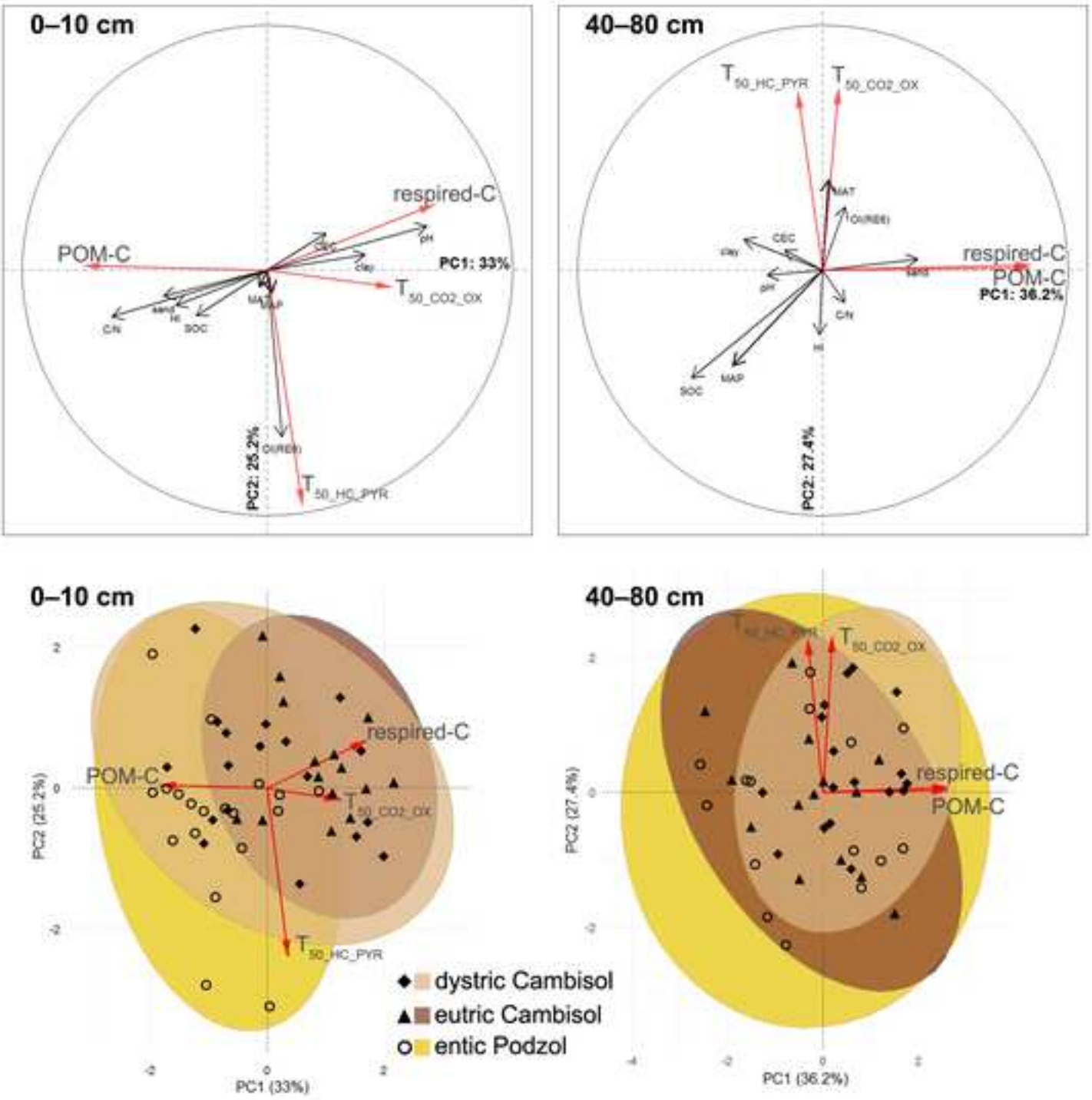

Supplementary material captions

Online Resource 1 Description of the Rock-Eval 6 thermal analysis (adapted from Baudin et al., 2017) and calculation of the two RE6-derived parameters (hydrogen index; $T_{50\_CO2\_OX}$, the temperature at which 50% of the residual SOM was oxidized to CO_2 during the oxidation phase)

Baudin F, Tribovillard N, Trichet J (2017) Géologie De La Matière Organique. EDP Sciences, Lilles, France.

Online Resource 2 Correlation between C content (%) of isovolumetrically pooled samples (measured in this study as detailed in *Materials and Methods* subsection a) and average values of the 5 replicates × 5 subplots from RENECOFOR samples (calculated with values from Jonard et al. (2017) and Ponette et al. (1997) for samples 0–40cm and 40–100 cm, respectively) for a given soil layer (n = 242). The 1:1 line has been added in red for reference

Jonard M, Nicolas M, Coomes DA, Caignet I, Saenger A, Ponette Q (2017) Forest soils in France are sequestering substantial amounts of carbon. Sci Total Environ 574:616-628

Ponette Q, Ulrich E, Brêthes A, Bonneau M, Lanier M (1997) RENECOFOR - Chimie des sols dans les 102 peuplements du réseau : campagne de mesures 1993-95. ONF, Département des recherches techniques, Fontainebleau, France

Online Resource 3 Details of models and their significant terms selected to explain variations in respired-C and POM-C, $T_{50\_HC\_PYR}$, and $T_{50\_CO2\_OX}$ in the 53 study plots (analysis by profile). All models used a gls function (see details in the *Calculations and statistical analyses* section)

Online Resource 4 Mean (and standard deviation) of the indicators of labile SOC ($T_{50\_HC\_PYR}$, POM-C; respired-C) and stable SOC ($T_{50\_CO2\_OX}$) for each soil class in the five different layers. The total SOC content was added for reference

Online Resource 5 Table of correlations for all samples and for each layer individually between the indicators of the SOC pools and the physico-chemical properties (SOC content, C/N ratio, HI, OIRE6, texture, pH, cationic exchange capacity), the climatic data of the plots (mean annual precipitation; MAP and mean annual temperature; MAT) and the chemical properties (C/N ratio) of the inputs and humus. Significance is indicated as follows: ***: $p < 0.001$; **: $p < 0.01$; *: $p < 0.05$. The high (> 0.6) correlations obtained with the SOC pools indicators are marked in bold. n = 242 total; n = 53 for layers 1 to 3 and n = 50 and n = 33 for layers 4 and 5 respectively unless specified otherwise

Online Resource 6 Distribution of the mean annual precipitation (MAP) and mean annual temperature (MAT) in the 53 study sites as a function of vegetation type illustrating a bias towards coniferous stands being in wetter and colder locations. n = 29 and 24 for coniferous and deciduous, respectively

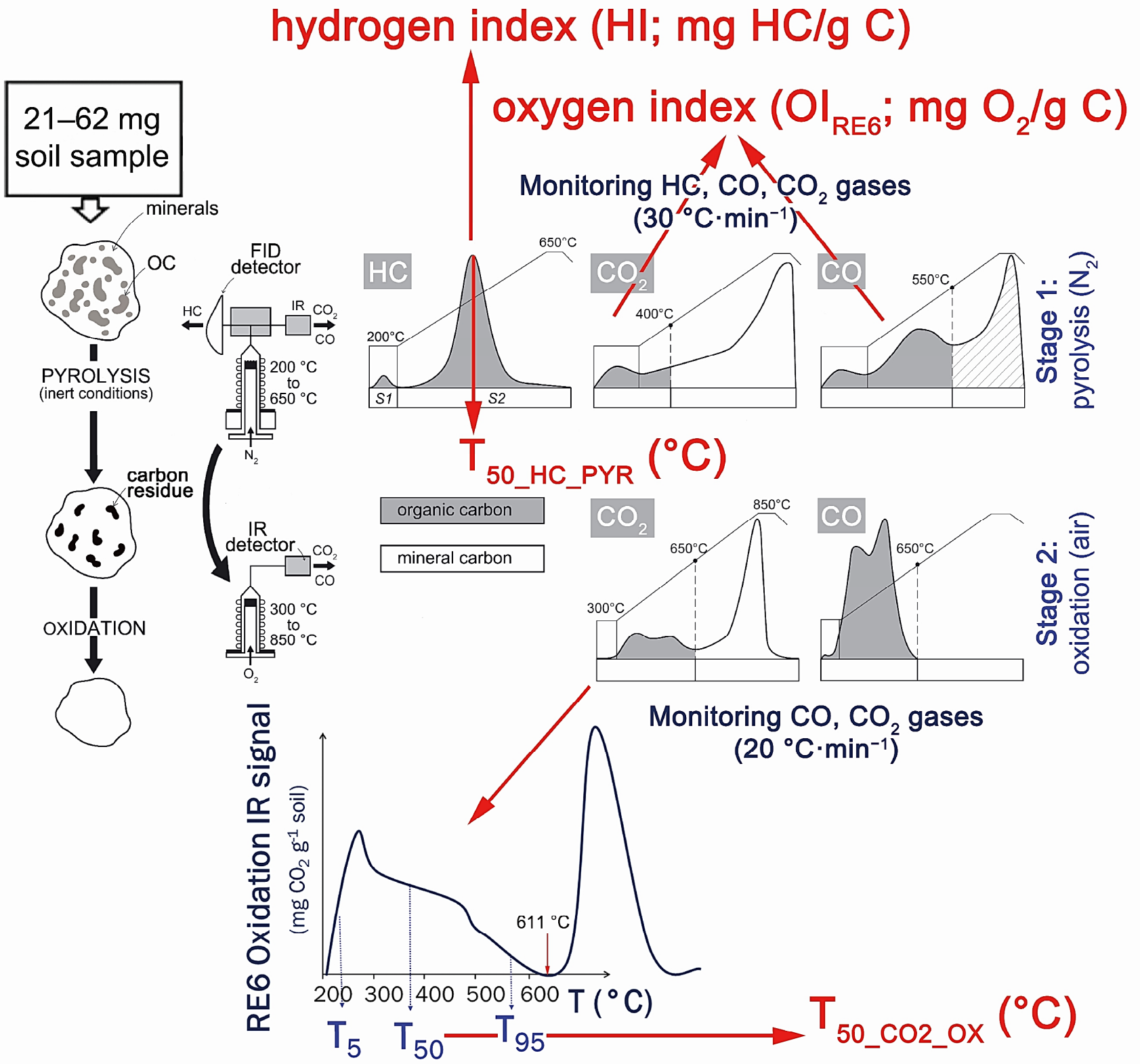
hydrogen index (HI; mg HC/g C)
oxygen index (OI$_{RE6}$; mg O$_2$/g C)
21–62 mg soil sample
minerals
OC
PYROLYSIS (inert conditions)
carbon residue
OXIDATION
FID detector
HC
IR
CO$_2$
CO
200 °C to 650 °C
N$_2$
IR detector
300 °C to 850 °C
O$_2$
Monitoring HC, CO, CO$_2$ gases (30 °C·min^{-1})
HC
CO$_2$
CO
200°C
400°C
550°C
650°C
S1
S2
Stage 1: pyrolysis (N$_2$)
T$_{50_HC_PYR}$ (°C)
organic carbon
mineral carbon
300°C
650°C
850°C
Stage 2: oxidation (air)
Monitoring CO, CO$_2$ gases (20 °C·min^{-1})
RE6 Oxidation IR signal
(mg CO$_2$ g^{-1} soil)
611 °C
200 300 400 500 600 T (°C)
T$_5$
T$_{50}$
T$_{95}$
T$_{50_CO2_OX}$ (°C)

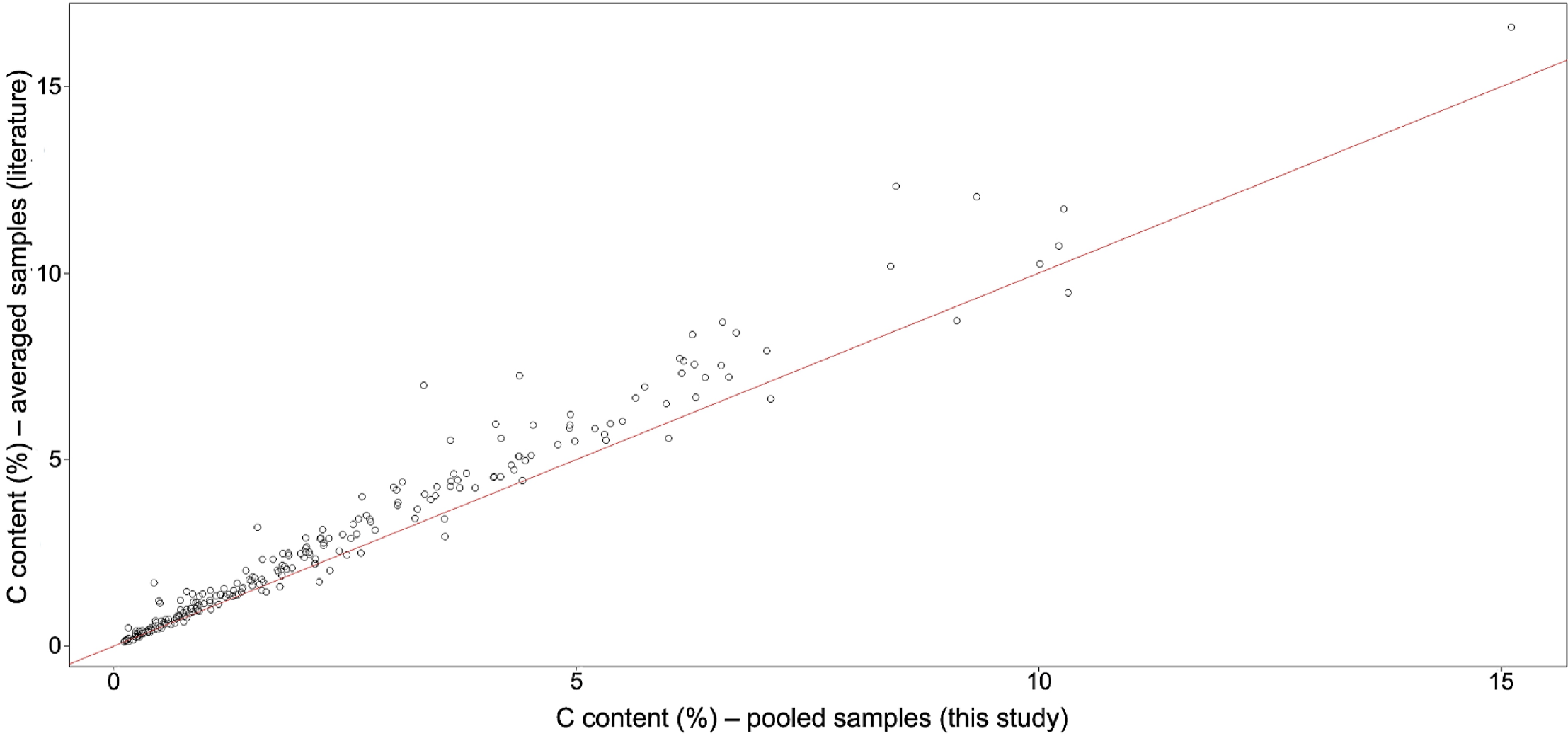
C content (%) – averaged samples (literature)
C content (%) – pooled samples (this study)
0
5
10
15
0
5
10
15

Online Resource 3 Details of models and their significant terms selected to explain variations in respired-C and POM-C, $T_{50\_HC\_PYR}$, and $T_{50\_CO2\_OX}$ in the 53 study plots (analysis by profile). All models used a gls function (see details in the *Calculations and statistical analyses* section)

Response variable	Transformation	Predictors in final model[$]	Level of significance *p*-value
respired-C	$\log_{10}$(respired-C + 1)	soil + depth + soil × depth	soil < 0.0001; depth =0.0823; depth × soil = 0.0417
POM-C	$\log_{10}$(POM-C)	depth + soil	depth < 0.0001 and soil = 0.0114
$T_{50\_HC\_PYR}$		depth + soil + veg + depth × soil + depth × veg + soil × veg	depth and depth × soil < 0.0001; soil = 0.1440; veg = 0.0665; depth × veg = 0.0023; soil × veg = 0.0236
$T_{50\_CO2\_OX}$		depth + veg + climate + depth × climate	all < 0.0001 except climate = 0.0272

[$] For all models, as a preliminary inspection of the variance of a given factor showed heterogeneity among the various layers, we used a constant variance function [varIdent(form= ~ 1 | depth)], which allowed five different variances, one for each soil layer. We also used the compound symmetry structure [corCompSymm(form =~ 1|plot)], which is similar to the variance structure of a random-intercept-only model. In our case, it allowed to treat each site as random factor.

Online Resource 4 Mean (and standard deviation) of the indicators of labile ($T_{50\_HC\_PYR}$, POM-C), very labile (respired-C) and stable SOC ($T_{50\_CO2\_OX}$) for each soil class in the five different layers. The basic soil physico-chemical properties (texture, total SOC content, C/N ratio and pH) were added for reference

layer	soil class	n	$T_{50\_HC\_PYR}$ (°C)		$T_{50\_CO2\_OX}$ (°C)		n	POM-C (% OC)		n	respired-C (µg CO_2-C·µg^{-1} soil C in %)		n	clay (%)		silt (%)		sand (%)		C content (%)		C/N ratio		pH	
0–10 cm	ALL	53	422	(8)	399	(8)	53	22.6	(7.3)	53	1.73	(0.57)	53	22	(14)	36	(18)	42	(29)	5.1	(2.7)	16.9	(4.5)	4.9	(1.0)
	dystric Cambisol	18	420	(8)	399	(8)	18	23.0	(7.5)	18	1.87	(0.70)	18	18	(9)	31	(14)	51	(21)	4.1	(1.8)	16.8	(3.4)	4.5	(0.3)
	eutric Cambisol	16	428	(7)	403	(10)	16	19.2	(5.6)	16	2.19	(0.62)	16	37	(11)	50	(13)	13	(20)	5.1	(1.9)	13.3	(1.5)	6.2	(0.9)
	entic Podzol	19	417	(9)	396	(8)	19	25.1	(7.6)	19	1.13	(0.38)	19	15	(9)	28	(19)	57	(25)	6	(3.6)	19.9	(5.0)	4.1	(0.2)
10–20 cm	ALL	53	434	(7)	408	(12)		nd		53	1.61	(0.56)	53	21	(13)	37	(18)	42	(29)	2.9	(2.0)	16.4	(4.9)	5.1	(1.1)
	dystric Cambisol	18	434	(8)	409	(10)		nd		18	1.54	(0.64)	18	17	(9)	32	(14)	51	(21)	1.9	(0.7)	16.3	(3.5)	4.6	(0.3)
	eutric Cambisol	16	435	(6)	410	(14)		nd		16	2.13	(0.74)	16	36	(11)	51	(11)	13	(17)	3.5	(1.6)	12.4	(1.1)	6.5	(1.0)
	entic Podzol	19	433	(8)	404	(11)		nd		19	1.15	(0.31)	19	13	(7)	29	(20)	58	(25)	3.3	(2.7)	19.8	(5.4)	4.3	(0.2)
20–40 cm	ALL	53	441	(7)	418	(15)		nd		53	1.43	(0.68)	53	20	(14)	36	(18)	43	(28)	1.8	(1.4)	14.8	(4.3)	5.4	(1.3)
	dystric Cambisol	18	444	(8)	421	(10)		nd		18	1.38	(0.61)	18	17	(9)	33	(14)	51	(21)	1.1	(0.4)	14.8	(3.8)	4.8	(0.3)
	eutric Cambisol	16	437	(5)	417	(16)		nd		16	1.86	(0.84)	16	35	(13)	48	(12)	17	(17)	2.4	(1.4)	11.3	(1.3)	7.2	(1.0)
	entic Podzol	19	443	(6)	417	(17)		nd		19	1.06	(0.58)	19	11	(6)	30	(20)	59	(25)	2.1	(1.8)	17.7	(4.3)	4.6	(0.1)
40–80 cm	ALL	50	448	(10)	431	(17)	50	11.5	(6.2)	46	1.34	(0.67)	50	20	(15)	32	(17)	48	(27)	0.8	(0.8)	11.6	(3.8)	5.8	(1.4)
	dystric Cambisol	18	449	(7)	438	(15)	18	13.3	(6.3)	17	1.48	(0.62)	18	18	(10)	28	(11)	54	(19)	0.5	(0.3)	10.5	(3.5)	5.1	(0.6)
	eutric Cambisol	14	444	(9)	424	(19)	14	7.8	(3.5)	14	1.51	(0.75)	14	35	(18)	41	(13)	24	(25)	0.9	(0.5)	9.3	(1.9)	7.9	(0.6)
	entic Podzol	18	450	(12)	430	(18)	18	12.5	(6.8)	15	1.03	(0.64)	18	11	(5)	28	(20)	62	(25)	1.1	(1.1)	14.6	(3.4)	4.8	(0.2)
80–100 cm	ALL	33	452	(13)	437	(17)		nd		31	1.17	(0.66)	33	22	(17)	34	(16)	44	(27)	0.6	(0.5)	9.7	(4.0)	6.1	(1.6)
	dystric Cambisol	11	450	(11)	445	(12)		nd		11	1.57	(0.91)	11	20	(11)	30	(12)	50	(19)	0.3	(0.2)	7.2	(1.9)	5.3	(1.0)
	eutric Cambisol	10	448	(11)	427	(16)		nd		10	1.14	(0.59)	10	38	(19)	41	(12)	21	(23)	0.7	(0.2)	8.4	(1.6)	8.2	(0.6)
	entic Podzol	12	458	(18)	439	(22)		nd		10	0.79	(0.49)	12	10	(4)	30	(21)	59	(23)	0.8	(0.7)	13.1	(4.6)	5.0	(0.4)
0–100 cm	ALL	242	439	(9)	419	(14)	103	17.2	(8.8)	236	1.46	(0.63)	242	21	(14)	35	(17)	44	(28)	2.4	(2.4)	14.2	(5.0)	5.4	(1.3)

Online Resource 5 Table of correlations for all samples and for each layer individually between the indicators of the SOC pools and the physico-chemical properties (SOC content, C/N ratio, HI, OI_{RE6}, texture, pH, cationic exchange capacity), the climatic data of the plots (mean annual precipitation; MAP and mean annual temperature; MAT) and the chemical properties (C/N ratio) of the inputs and humus. Significance is indicated as follows: ***: $p < 0.001$; **: $p < 0.01$; *: $p < 0.05$. The high (> 0.6) correlations obtained with the SOC pools indicators are marked in bold. n = 242 total; n = 53 for layers 1 to 3 and n = 50 and n = 33 for layers 4 and 5 respectively unless specified otherwise

	POM-C[§]	respired-C[*]	$T_{50\_HC\_PYR}$	$T_{50\_CO2\_OX}$	SOC	C/N ratio (soil)	HI	OI_{RE6}	Clay	Sand	pH_{water}	CEC	MAP	MAT	C/N ratio (inputs)
respired-C	0.20														
$T_{50\_HC\_PYR}$	**−0.73*** **	−0.32***													
$T_{50\_CO2\_OX}$	−0.56***	−0.15*	**0.67*** **												
SOC	0.52***	0.03	−0.58***	**−0.72*** **											
C/N ratio (soil)	**0.61*** **	−0.13*	−0.34***	−0.43***	0.42***										
HI	**0.67*** **	0.08	**−0.67*** **	−0.53***	0.58***	0.62***									
OI_{RE6}	**−0.76*** **	−0.04	**0.63*** **	0.50***	−0.56***	−0.78***	−0.84***								
Clay	−0.18	0.19**	−0.06	−0.03	0.31***	−0.51***	−0.16*	0.31***							
Sand	0.18	−0.15*	0.02	0.10	−0.32***	0.45***	0.14*	−0.28***	−0.89***						
pH_{water}	−0.54***	0.23***	0.31***	0.33***	−0.22***	−0.61***	−0.45***	0.59***	0.44***	−0.45***					
CEC	0.08	0.31***	−0.33***	−0.25***	0.48***	−0.31***	0.14*	0.06	0.74***	−0.69***	0.47***				
MAP	−0.11	−0.16*	0.06	−0.20**	0.36***	−0.01	−0.06	0.12	0.14*	−0.17**	0.07	0.12			
MAT	−0.02	−0.09	0.01	0.19**	−0.25***	−0.02	0.13*	−0.11	−0.08	0.06	−0.22***	−0.22***	−0.60***		
C/N ratio (inputs)	0.22*	0.16*	−0.09	−0.16*	−0.07	0.24***	−0.05	−0.06	−0.24***	0.23***	−0.03	−0.17**	−0.24***	−0.08	
C/N ratio (humus)	0.01	0.38***	−0.14*	−0.11	−0.01	−0.03	−0.08	0.10	0.12	−0.14*	0.40***	0.18**	−0.05	−0.06	0.44***

[§] n = 99 [*] n = 236

LAYER 1: 0–10 cm

	POM-C	respired-C	$T_{50\_HC\_PYR}$	$T_{50\_CO2\_OX}$	SOC	C/N ratio (soil)	HI	OI_{RE6}	Clay	Sand	pH_{water}	CEC	MAP	MAT	C/N ratio (inputs)
respired-C	−0.29*														
$T_{50\_HC\_PYR}$	−0.44***	0.12													
$T_{50\_CO2\_OX}$	−0.19	0.13	0.45***												
SOC	0.17	−0.20	−0.10	−0.28*											
C/N ratio (soil)	0.56***	−0.51***	−0.55***	−0.19	−0.08										
HI	0.32*	−0.43**	−0.30*	0.07	−0.29*	0.67***									
OI_{RE6}	−0.41**	0.52***	0.40**	−0.06	0.25	−0.80***	−0.91***								
Clay	−0.29*	0.43**	0.44**	−0.03	0.44**	−0.70***	−0.71***	0.75***							
Sand	0.32*	−0.41**	−0.50***	−0.08	−0.32*	0.65***	0.61***	−0.65***	−0.88***						
pH_{water}	−0.35**	**0.62*** **	0.46***	0.36**	0.06	−0.70***	−0.61***	0.70***	0.60***	−0.62***					
CEC	−0.16	0.30*	0.35*	0.00	0.60***	−0.60***	−0.72***	0.72***	0.78***	−0.72***	0.64***				
MAP	−0.10	0.10	−0.11	−0.29*	0.53***	−0.25	−0.37**	0.35*	0.33*	−0.21	0.06	0.39**			
MAT	−0.09	−0.30*	0.14	0.25	−0.39**	0.10	0.32*	−0.30*	−0.26	0.13	−0.21	−0.45***	−0.61***		
C/N ratio (inputs)	0.31*	−0.03	−0.41**	−0.25	−0.07	0.47***	−0.02	−0.13	−0.26	0.28*	−0.14	−0.16	−0.25	−0.06	
C/N ratio (humus)	−0.04	0.47***	−0.10	0.10	−0.17	−0.07	−0.41**	0.34*	0.11	−0.16	0.42**	0.14	−0.05	−0.07	0.45***

LAYER 2: 10–20 cm

	POM-C	respired-C	$T_{50\_HC\_PYR}$	$T_{50\_CO2\_OX}$	SOC	C/N ratio (soil)	HI	OI_{RE6}	Clay	Sand	pH_{water}	CEC	MAP	MAT	C/N ratio (inputs)
respired-C	nd														
$T_{50\_HC\_PYR}$	nd	0.00													
$T_{50\_CO2\_OX}$	nd	0.02	0.40**												
SOC	nd	−0.13	0.08	−0.09											
C/N ratio (soil)	nd	−0.33*	−0.13	−0.04	−0.34*										
HI	nd	−0.24	−0.26	0.14	−0.28*	0.60***									
OI_{RE6}	nd	0.34*	0.21	−0.22	0.37**	−0.73***	−0.74***								
Clay	nd	0.29*	0.10	0.07	0.60***	−0.71***	−0.53***	0.65***							
Sand	nd	−0.29*	−0.12	−0.05	−0.52***	0.66***	0.44**	−0.58***	−0.88***						
pH_{water}	nd	**0.60*** **	0.08	0.29*	0.28*	−0.62***	−0.36**	0.51***	0.59***	−0.58***					
CEC	nd	0.27*	0.13	−0.01	0.73***	−0.65***	−0.40**	0.60***	0.76***	−0.77***	0.64***				
MAP	nd	−0.08	−0.06	−0.24	0.66***	−0.20	−0.17	0.23	0.30*	−0.24	0.10	0.39**			
MAT	nd	−0.20	−0.05	0.21	−0.47***	0.12	0.25	−0.29*	−0.20	0.12	−0.27	−0.42**	−0.61***		
C/N ratio (inputs)	nd	0.20	−0.05	−0.25	−0.21	0.32*	−0.12	0.02	−0.26	0.28*	−0.05	−0.23	−0.25	−0.06	
C/N ratio (humus)	nd	0.53***	−0.12	−0.01	−0.02	−0.14	−0.22	0.27*	0.14	−0.15	0.51***	0.11	−0.05	−0.07	0.45***

LAYER 3: 20–40 cm

	POM-C	respired-C	$T_{50\_HC\_PYR}$	$T_{50\_CO2\_OX}$	SOC	C/N ratio (soil)	HI	OI_{RE6}	Clay	Sand	pH_{water}	CEC	MAP	MAT	C/N ratio (inputs)
respired-C	nd														
$T_{50\_HC\_PYR}$	nd	−0.33*													
$T_{50\_CO2\_OX}$	nd	0.06	0.37**												
SOC	nd	−0.21	−0.12	−0.41**											
C/N ratio (soil)	nd	−0.27	0.21	0.06	−0.15										
HI	nd	−0.10	−0.21	0.05	0.13	0.48***									
OI_{RE6}	nd	0.11	−0.05	−0.31*	0.20	−0.76***	−0.65***								
Clay	nd	0.29*	−0.22	−0.04	0.46***	−0.74***	−0.34*	0.70***							
Sand	nd	−0.23	0.21	0.15	−0.48***	0.68***	0.24	−0.64***	−0.90***						
pH_{water}	nd	0.45***	−0.32*	−0.15	0.29*	−0.47***	−0.11	0.40**	0.54***	−0.50***					
CEC	nd	0.19	−0.30*	−0.24	0.62***	−0.59***	−0.13	0.51***	0.77***	−0.76***	0.65***				
MAP	nd	−0.15	0.02	−0.38**	0.72***	−0.05	0.10	0.11	0.20	−0.25	0.07	0.31*			
MAT	nd	0.00	−0.07	0.33*	−0.49***	0.03	0.16	−0.25	−0.16	0.13	−0.26	−0.35**	−0.61***		
C/N ratio (inputs)	nd	0.04	0.12	−0.16	−0.26	0.26	−0.25	0.00	−0.25	0.27	0.10	−0.27	−0.25	−0.06	
C/N ratio (humus)	nd	0.41**	−0.26	−0.19	−0.02	−0.09	−0.17	0.19	0.13	−0.11	0.59***	0.14	−0.05	−0.07	0.45***

LAYER 4: 40–80 cm

	POM-C	respired-C*	$T_{50\_HC\_PYR}$	$T_{50\_CO2\_OX}$	SOC	C/N ratio (soil)	HI	OI_{RE6}	Clay	Sand	pH_{water}	CEC	MAP	MAT	C/N ratio (inputs)
respired-C	0.47***														
$T_{50\_HC\_PYR}$	−0.35*	−0.41**													
$T_{50\_CO2\_OX}$	−0.01	−0.01	0.19												
SOC	−0.43**	−0.54***	0.21	−0.49***											
C/N ratio (soil)	0.30*	−0.17	0.13	−0.21	0.29*										
HI	0.06	−0.03	−0.21	−0.24	0.19	0.23									
OI_{RE6}	−0.42**	0.13	0.11	0.22	−0.07	−0.65***	−0.43**								
Clay	−0.34*	−0.08	0.03	0.12	0.33*	−0.55***	−0.06	0.62***							
Sand	−0.42**	0.16	−0.12	0.10	−0.48***	0.44**	0.04	−0.51***	−0.90***						
pH_{water}	0.46***	0.03	−0.02	−0.18	0.20	−0.27	0.09	0.28	0.36*	−0.36*					
CEC	−0.34*	0.13	−0.08	−0.02	0.25	−0.49***	0.05	0.52***	0.80***	−0.75***	0.66***				
MAP	−0.25	−0.42**	0.16	−0.45**	0.69***	0.36*	0.17	−0.13	−0.03	−0.12	−0.04	−0.07			
MAT	0.04	0.09	0.13	0.50***	−0.48***	−0.28*	0.03	0.16	0.08	0.01	−0.15	−0.06	−0.58***		
C/N ratio (inputs)	0.33*	0.30*	−0.19	−0.22	−0.15	0.21	−0.08	−0.12	−0.31*	0.26	0.01	−0.26	−0.24	−0.11	
C/N ratio (humus)	0.10	0.29	−0.27	−0.29*	0.02	0.13	0.01	0.11	0.00	−0.06	0.37**	0.15	−0.04	−0.10	0.44**

* n = 46

LAYER 5: 80–100 cm

	POM-C	respired-C*	$T_{50\_HC\_PYR}$	$T_{50\_CO2\_OX}$	SOC	C/N ratio (soil)	HI	OI_{RE6}	Clay	Sand	pH_{water}	CEC	MAP	MAT	C/N ratio (inputs)
respired-C	nd														
$T_{50\_HC\_PYR}$	nd	−0.48**													
$T_{50\_CO2\_OX}$	nd	−0.12	0.08												
SOC	nd	−0.43*	0.34	**−0.69*****											
C/N ratio (soil)	nd	−0.30	0.37*	−0.26	0.39*										
HI	nd	0.17	−0.39*	−0.30	0.04	0.00									
OI_{RE6}	nd	0.31	−0.18	0.25	−0.29	−0.58***	−0.14								
Clay	nd	−0.10	−0.11	0.02	0.14	−0.51**	0.09	0.38*							
Sand	nd	0.09	−0.06	0.17	−0.30	0.41*	−0.06	−0.29	−0.86***						
pH_{water}	nd	−0.01	−0.03	−0.46**	0.39*	−0.12	0.22	−0.18	0.36*	−0.37*					
CEC	nd	0.27	−0.36*	−0.13	0.04	−0.36*	0.30	0.21	0.72***	−0.60***	0.64***				
MAP	nd	−0.21	0.26	−0.34	0.60***	0.46**	0.05	−0.11	−0.30	0.10	0.04	−0.24			
MAT	nd	−0.12	0.09	0.43*	−0.43*	−0.27	0.13	0.29	0.27	−0.17	−0.24	0.03	−0.54**		
C/N ratio (inputs)	nd	0.45*	−0.12	−0.20	−0.01	−0.08	−0.21	0.13	−0.09	−0.05	−0.03	−0.06	−0.12	−0.13	
C/N ratio (humus)	nd	0.25	−0.07	−0.22	0.13	0.02	0.04	0.14	0.27	−0.34	0.14	0.25	−0.06	0.05	0.41*

* n = 31

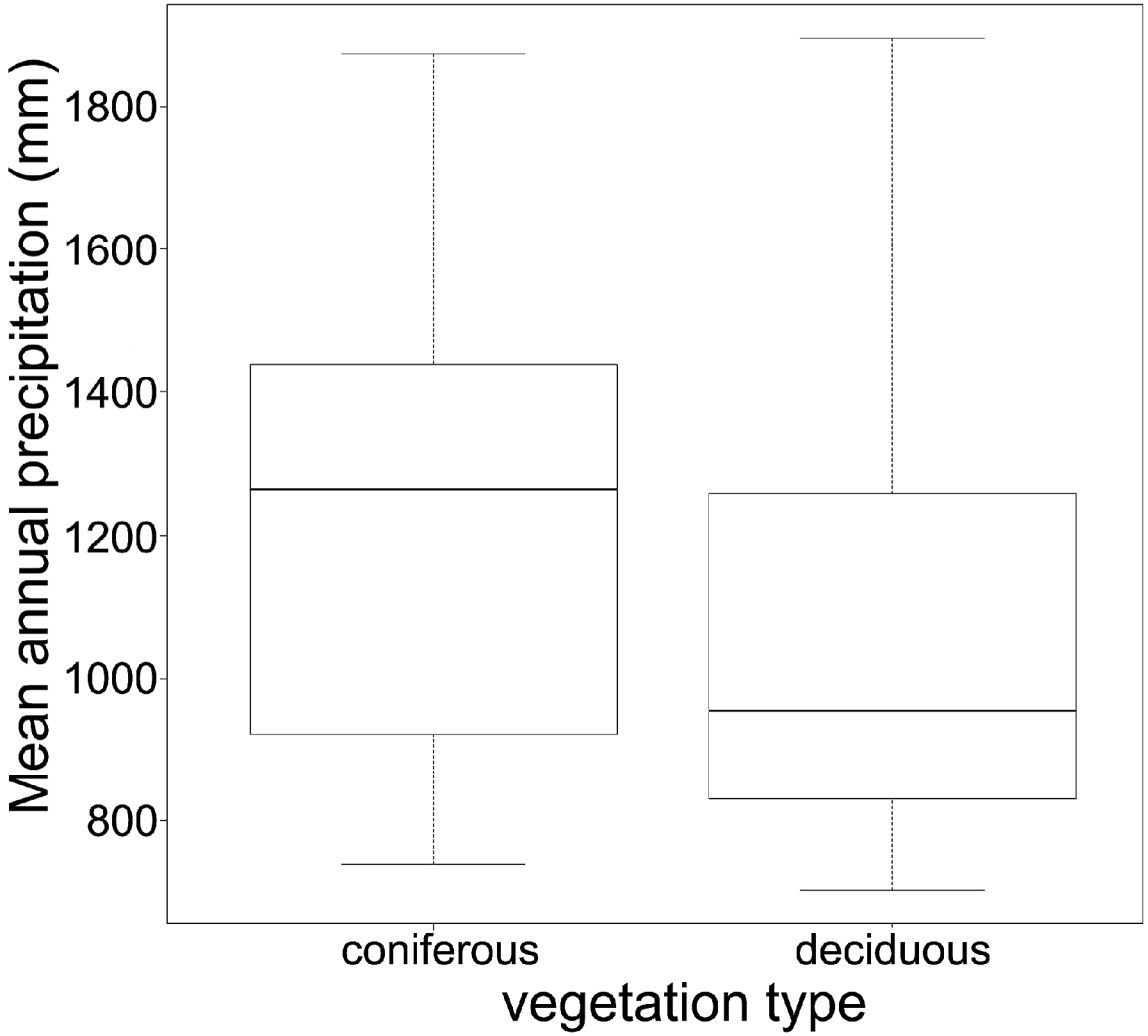
Mean annual precipitation (mm)
1800
1600
1400
1200
1000
800
coniferous
deciduous
vegetation type

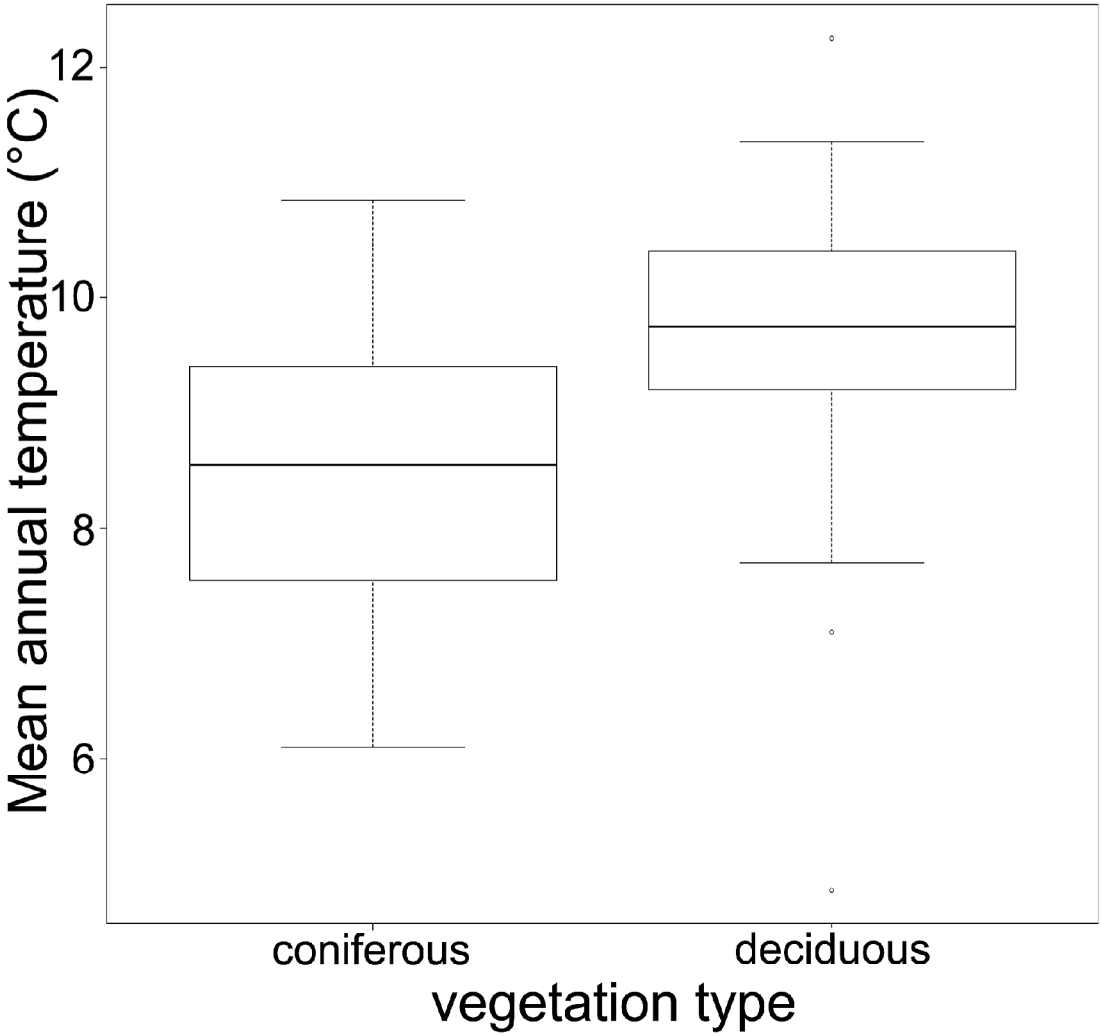
Mean annual temperature (°C)
12
10
8
6
coniferous
deciduous
vegetation type